Bull Volcanol (2012) 74:1985–2005
DOI 10.1007/s00445-012-0643-8

RESEARCH ARTICLE

Stratigraphy, geochronology and evolution of the Mt. Melbourne volcanic field (North Victoria Land, Antarctica)

Guido Giordano · Federico Lucci · David Phillips · Domenico Cozzupoli · Valentina Runci

Received: 24 May 2012 / Accepted: 24 July 2012 / Published online: 15 August 2012

Abstract Mt. Melbourne (2,732 m a.s.l.) is a large quiescent stratovolcano located in Northern Victoria Land (Antarctica) and is one of a handful of volcanoes on the Antarctic plate with the potential for large-scale explosive eruptions. During the XVIII Italian Expedition in 2002–2003, the Mt. Melbourne volcanic succession was studied in terms of stratigraphy and sampled for $^{40}Ar/^{39}Ar$ age determinations and geochemistry. The early, Lower Pleistocene, volcanism was largely alkali basaltic to hawaiitic in composition and monogenetic in style, producing tens of small scoria cones and lava flows scattered over a wide area across the Transantarctic Mountains (Random Hills Period). During the Middle Pleistocene, volcanic activity focused to the area of the Mt. Melbourne stratovolcano, where several monogenetic centres show the transition from early subglacial/subaqueous conditions to emergent subaerial conditions (Shield Nunatak Period). The oldest exposed deposit associated with the early activity of the Mt. Melbourne stratovolcano (Mt. Melbourne Period) is a trachytic subaerial ignimbrite dated at 123.6±6.0 ka, which reflects the establishment of a crustal magma chamber. Above the ignimbrite a succession of alkali basaltic, hawaiitic, and subordinate benmoreitic lavas and scoria cones is exposed, dated at 90.7±19.0 ka. The Holocene deposits are exposed at the top of Mt. Melbourne, where the crater rim is composed of trachytic to rhyolitic pumice fall deposits, which are also extensively dispersed around the volcano, likely originated from Plinian-scale eruptions. The most recent explosive deposit proved difficult to date accurately because very low quantities of radiogenic ^{40}Ar were released, resulting in imprecise plateau ages of 50±70 and 35±22 ka.

Keywords Antarctica · Explosive volcanism · Geochronology · Mt. Melbourne · Geochemistry

Editorial responsibility: J.D.L. White

Electronic supplementary material The online version of this article (doi:10.1007/s00445-012-0643-8) contains supplementary material, which is available to authorized users.

G. Giordano (✉) · F. Lucci · D. Cozzupoli · V. Runci
Dipartimento di Scienze Geologiche,
Università degli Studi Roma Tre,
Largo S. Leonardo Murialdo 1,
00146 Rome, Italy
e-mail: giordano@uniroma3.it

D. Phillips
Department of Geological Sciences, Melbourne University,
Melbourne, Victoria, Australia

Introduction

Ash produced from the 2010 trachyandesitic explosive eruption of Iceland's Eyjafjallajökull volcano caused major disruption to air travel in the northern hemisphere, resulting in significant economic losses to the global economy. More recently, ash produced by Chile's Puyehue-Cordón Caulle volcano, in 2011, circled the globe at high latitude, disrupting air traffic in the southern hemisphere, with significant impact on local economies. These events highlight the importance of scientific assessment of the explosive potential of volcanoes, globally, which may have the capacity to produce upper atmospheric ash clouds that can be widely dispersed by atmospheric circulation. Intra-plate volcanoes in Antarctic are among the candidates with the potential for major explosive activity; however, the hazard level of those volcanoes is yet to be fully determined, largely because Antarctic volcanoes are extensively ice-covered, and documentation of their volcanic rock sequences is both challenging and time-consuming.

Late Cenozoic intra-plate volcanoes in Antarctica are mostly associated with rift zones such as the extensive West Antarctic Rift System (Behrendt 1999). Antarctic volcanoes are typically alkaline, ranging from basaltic to phonolitic and trachytic in composition. Most volcanoes have erupted

largely effusively, although explosive eruptions are known from magma–ice interactions and/or associated with the most evolved compositions (LeMasurier and Thomson 1990). Holocene felsic pyroclastic deposits dispersed regionally from Plinian-scale eruptions are known from Mt. Takahe and Mt. Berlin (Wilch et al. 1999; Dunbar et al. 2008). Other quiescent potentially explosive volcanoes include Mt. Melbourne and Mt. Rittman in Northern Victoria Land; this assessment is based on evidence for recent activity, such as the presence of ash layers on ice, age determinations, and the presence of fumarolic activity (see LeMasurier and Thomson 1990 for a complete list; see also the Smithsonian Institute website).

During the "Austral summer 2002–2003", the Italian XVIII Expedition to Northern Victoria Land (Antarctica) included a detailed field study of the Mt. Melbourne Volcanic Province (Kyle 1990a). This field study built on previous work published by New Zealand, German and Italian parties, in the 1960s, 1970–1980s and 1980–1990s, respectively (Nathan and Schulte 1967, 1968; Kyle and Cole 1974; Lyon and Giggenbach 1974; Lyon 1986; Wörner and Viereck 1989; Wörner et al. 1989; Rocchi et al. 2003; Armienti et al. 1991; Beccaluva et al. 1991a, b; Lanzafame and Villari 1991; Salvini et al. 1997; Rossetti et al. 2000; Storti et al. 2006).

This paper presents a detailed reconstruction of the lithostratigraphic architecture of the volcanic successions of the Mt. Melbourne stratovolcano and the surrounding volcanic sequences. A set of stratigraphically controlled samples have provided new $^{40}Ar/^{39}Ar$ age determinations and allowed definition of the magma compositional variation, which together have allowed us to reconstruct the evolution of the volcanism in the region and, in particular, the history of Mt. Melbourne stratovolcano, in terms of eruptive styles and the potential for future explosive eruptions.

Geological framework and previous studies

The Mt. Melbourne volcanic field belongs to the Tertiary to Quaternary alkaline volcanoes of Northern Victoria Land (Fig. 1), which form part of the McMurdo Volcanic Group (Harrington 1958; Kyle 1990b) and are closely related to the transtensional tectonic evolution of the Transantarctic Mountains–Ross Sea basin system (Salvini et al. 1997; Rossetti et al. 2000; Rocchi et al. 2003). This volcanism forms one of the most extensive alkali volcanic provinces in the world, with a geographic extent comparable to that of alkaline rocks in the East African Rift (Kyle 1990b). Magmatism in the region initiated at about 50 Ma associated with the extension of the Ross Sea Basin and became more intense after about 30 Ma when the major NE-trending faults in the area were re-activated with right-lateral strike–slip kinematics (Salvini et al. 1997; Rossetti et al. 2000; Rocchi et al. 2003; Storti et al. 2006). Recently, Lesti et al. (2008) proposed a relationship between the Cenozoic magmatism of southeast Australia and the contemporaneous activity in Northern Victoria Land. These authors suggested that transtension associated with the Tasman Zone transform may have been responsible for the generation and eruption of magma across passive margins, in agreement with the model proposed by Salvini et al. (1997).

The volcanic edifices of the McMurdo Volcanic Group include both scattered monogenetic scoria cones and lava flows, and larger shield volcanoes and stratovolcanoes (LeMasurier and Thomson 1990). Basaltic shield volcanoes formed close to the coast, i.e. close to the Ross Sea Basin shoulder. Examples include the 70×20 km Cape Adare system, Coulman Island and Cape Washington (LeMasurier and Thomson 1990). Stratovolcanoes are characterised by more differentiated trachytic to phonolitic compositions, such as at Mt. Morning (Martin et al. 2010), Mt. Overlord, Mt. Rittmann, Berlin dome, Mt. Melbourne and Mt. Erebus (LeMasurier and Thomson 1990). Kyle and Cole (1974) subdivided the McMurdo Volcanic Group into informal provinces that include, from north to south, the Hallett, Melbourne and Erebus volcanic provinces. These volcanic provinces are based on the spatial distribution, tectonic setting and petrographic characteristics of volcanoes in the region. The Mt. Melbourne Volcanic Province (MMVP) is associated with a series of major NE-trending dextral faults, which cross-cut the Transantarctic Mountains (Fig. 1), connecting with the N–S trending extensional faults of the Ross Sea basin (Rossetti et al. 2000). The MMVP includes several large stratovolcanoes composed of felsic rocks, such as trachytes and peralkaline trachytes. These rocks exceed in volume the more basic rocks such as alkali basalts, basanites and hawaiites (LeMasurier and Thomson 1990). The main volcanic fields are the Malta Plateau and The Pleiades to the north, Mount Overlord in the centre and Mount Melbourne in the south.

Mt. Melbourne

Mt. Melbourne (74.35° S; 164.70° E) is a stratovolcano located between the Tinker Glacier and the Campbell Glacier (Fig. 1). The volcano is elongate NNE (Fig. 1) along the main structural fabric of the basement. The total volume of the volcano's cone was calculated at 180 km^3 for the summit cone plus 250 km^3 in the surrounding volcanic field (Worner and Viereck 1990). The volcano is quiescent, with fumarolic activity at the summit crater (2,732 m above sea level), where the temperature of the gas is constant at 59 °C, just 25 cm below the ice cap (Nathan and Schulte 1967; Keys et al. 1983; Cremisini et al. 1991). Furthermore, the undissected cone morphology and widespread pumice fall

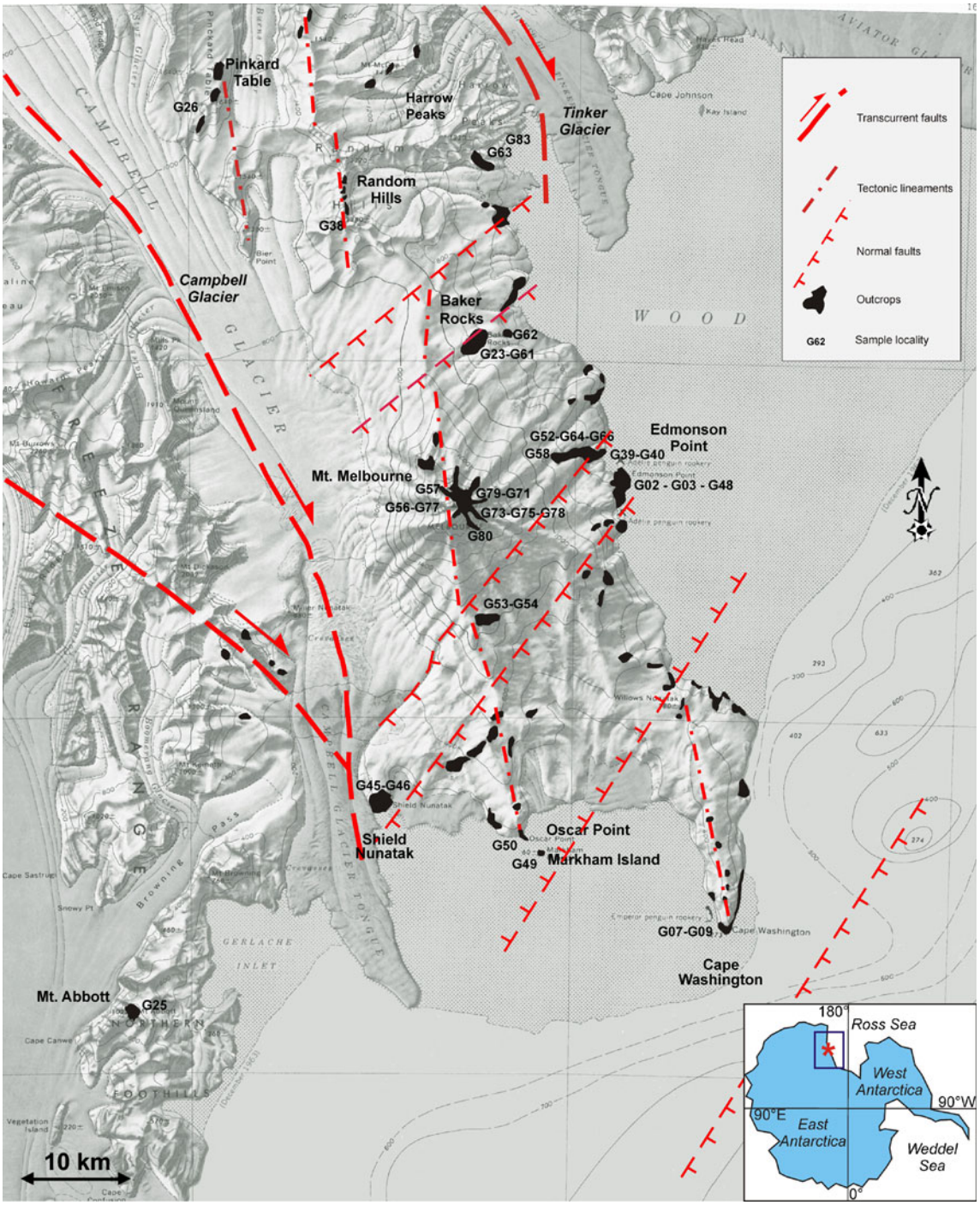

Fig. 1 Shaded topography of the Mt. Melbourne volcanic region. The *numbers* indicate the location of selected samples (see Appendix 1 for geographic coordinates) analysed in this study for geochemistry and age determinations. The main fault systems are from Storti et al 2006. The *red box in the inset* locates Mt. Melbourne in the Antarctic continent

layers, located only a few centimetres below the surface of the ice cap, have been reported as evidence of recent explosive activity (e.g. Wörner and Viereck 1989). The youngest age determination obtained for recent deposits is 0.01± 0.02 Ma (Armstrong 1978). However Lyon (1986), based on the depth within the ice cap at which tephra layers from the most recent explosive activity at Mt. Melbourne were found, proposed that the most recent eruption probably occurred between 1862 and 1922.

Previous detailed work on the Mt. Melbourne volcanic products includes the results of the German GANOVEX party (Wörner and Viereck 1989; Wörner et al. 1989), and

those of the II Italian Expedition (Armienti and Tripodo 1991; Armienti et al. 1991; Beccaluva et al. 1991a, b; Hornig et al. 1991; Lanzafame and Villari 1991; Müller et al. 1991). The Mt. Melbourne volcanic products overlie the Precambrian–Ordovician intrusive and metamorphic basement rocks of the Wilson Terrane. They range from effusive to explosive and erupted from subaerial to subaqueous/subglacial environments (Wörner and Viereck 1989). The main compositions range from basanite, alkali basalt and hawaiite to more evolved comenditic trachyte varieties (Wörner et al. 1989; Beccaluva et al. 1991b; Armienti et al. 1991; Antonini et al. 1994).

Published age data are all K/Ar determinations (Table 1 and Appendix 5) and suggest that the monogenetic volcanoes surrounding Mt. Melbourne to the north, across the Transantarctic Mountains, are Miocene-Pliocene in age (about 12–3 Ma; Armienti et al. 1991). To the south of Mt. Melbourne, the remnants of the N-trending Cape Washington basaltic shield (Fig. 1) yielded younger ages between 2.7 and 1.67 Ma (Kreutzer, 1988, unpublished report, quoted in Wörner and Viereck 1989). All available ages for the Mt. Melbourne stratovolcano itself are Quaternary (see data compilation in Kyle 1990a). Unfortunately several published ages are either quotations from unpublished reports (e.g. Kreutzer, 1988) or they are not supported by sample descriptions, sampling localities, or analytical details (e.g. Armienti et al. 1991). Furthermore, some published ages related to the same volcanic units are discordant (e.g. ages of Shield Nunatak in Table 1). In addition, none of the reported age determinations indicate the level of uncertainty in the listed errors (1σ or 2σ). It is clear therefore that new, stratigraphically controlled $^{40}Ar/^{39}Ar$ data are essential to describe the evolution of the Mt. Melbourne volcanic area.

Stratigraphy

The stratigraphy and physical characteristics of the volcanic products are described for the following areas: the Mt. Melbourne stratovolcano, the Mt. Melbourne peripheral centres and the monogenetic volcanic field distributed across the Transantarctic Mountains. Samples from 33 localities were collected for geochemical and geochronological analyses (Fig. 1 and Appendix 1).

The Mt. Melbourne stratovolcano

Edmonson Point (0 m a.s.l.) to 723 m a.s.l

Edmonson Point is located along the coast to the east of the summit and reveals the lowest part of the exposed stratigraphy of the Mt. Melbourne stratovolcano (Figs. 1 and 2). The area is characterised by two headlands, a promontory to the south and exposed cliffs to the north (Edmonson Point S and Edmonson Point N respectively), separated by the Edmonson Point glacier tongue (Baroni and Orombelli 1994). Some of the localities in the area have been described by Wörner and Viereck (1989). Despite some ice-covered sections, the area offers an almost continuous stratigraphic section from sea level up to the elevation of 723 m a.s.l. (Fig. 2), with excellent exposures that allow reconstruction of the complete stratigraphic succession. The succession is subdivided into five distinctive rock formations, described in stratigraphic order (Fig. 2).

Edmonson Point trachytic ignimbrite (EPI) The EPI unit is exposed along the base of the coastal cliffs of Edmonson Point S (Figs. 2 and 3). The maximum thickness in outcrop is 30 m, but the base of the EPI is not exposed. There are two main outcrops, each about 200 m long, displaying very similar facies over more than 1 km. The ignimbrite comprises three main lithostratigraphic sub-units, with depositional surfaces dipping 35° SW. Several faults produce local displacements of several decimetres and are associated with the later intrusion of dykes (Fig. 3a). The lower sub-unit is a 15-m-thick, white-pumice lapilli-rich (30–40 vol%, $Ø_{max}$ 2–4 cm), ash-matrix supported (40 vol%), massive and chaotic deposit, with abundant accessory lithics (10–20 vol%, $Ø_{max}$ 8 cm). The white pumice (sample G03, Appendixes 6 and 7) is vesicular, poorly porphyritic and contains phenocrysts of sanidine (59–61 % Ab), and hedenbergite (48 % Wo, <1 % En and 51 % Fs). A matrix-supported breccia lens is embedded in the lower sub-unit with gradational contacts (Fig. 3b). The breccia is composed of angular to subrounded lithic fragments, up to 60 cm in diameter. Clast types include (a) pale grey, poorly porphyritic (sanidine and amphibole) microcrystalline lava of likely trachytic composition (30–40 % of relative abundance); (b) black, scoriaceous, porphyritic lava (plagioclase and pyroxene) of likely basaltic composition (20–30 %); (c) homogeneous to banded syenite (5 %); and (d) reddish, hydrothermally altered clasts of basement gneiss (5–10 %). Above the breccia lens, the lower ignimbrite sub-unit contains coexisting white-pumice and black, sanidine-phyric vesicular-pumice lapilli. The middle sub-unit is a 2-m-thick succession of moderately sorted, rounded pumice lapilli-rich and plane parallel to low-angle cross-stratified beds probably of surge origin. The upper sub-unit is about 13 m thick, black-pumice-lapilli-rich (30–40 vol%, $Ø_{max}$ 10 cm), ash-matrix-supported (60–70 vol%), lithic-poor, massive and chaotic deposit. The pumice (sample G48, Appendixes 6 and 7) is black, highly vesicular, porphyritic, spatter-like, and contains Na-sanidine (Ab 55–61 %), andesine (An 46–47 %), fayalite (Fo 1–2 %) and Fe-hedenbergite (47–48 % Wo, 1–2 % En and 48–52 % Fs) crystals. The EPI ignimbrite was previously interpreted by Wörner and Viereck (1989) and by

Table 1 Summary of 40Ar/39Ar geochronology results from Mt. Melbourne and surrounding area: all uncertainties are listed at the 95 % confidence level

Area	Locality	Rock type	Sample number	Sample type	Plateau age (ka)	MSWD	Mean age (ka)	MSWD	Isochron age (ka)	MSWD	$^{40}Ar/^{36}Ar$ ratio	Previous ages (K/Ar, Ma)
Mt. Melbourne	Summit crater (recent lavas)	Grey porphyritic (snd, cpx) dense trachiti spatter	G77	K-Feldspar	50.0±70.0 (2σ)	0.7	–	–	–		–	Armstrong 1978:
		Brown porphyritic (snd, cpx) trachytic pumice	G79	K-Feldspar	35.1±21.9 (2σ)	1.4	–	–	61.6±66.4 (95 %)	3.6	297.6±6.4	0.01±0.02; 0.26±0.06; 0.08±0.015; Kreutzer 1988: 0.015±0.035
Mt. Melbourne Slope< 1,000 m.a.s.l.	Edmonson Point (ARL Lavas)	Black ropy porphyritic (pl, ol, amph) basalt	G52	Whole rock	–	–	111.6±83.8 (2σ)	0.6	37±88 (2σ)	0.3	299.4±4.2	
	Edmonson Point (ARL Lavas)	Black porphyritic (pl, ol) hawaiite	G39	Whole rock	–	–	297.6±55.4 (2σ)	1.2	-32±183 (2σ)	0.5	305.8±5.1	Kreutzer 1988:
		Grey porphyritic lava	G66	Plagioclase	90.7±19.0 (2σ)	1.0	–	–	94.4±25.8 (95 %)	1.5	299.4±3.9	0.05±0.02; 0.074±0.11
	Edmonson Point (EPI Ignimbrite)	Black porphyritic (snd, pl, ol, cpx) trachiti pumice	G48	K-Feldspar	–		118.6±11.6 (95 %)	2.8	103.3±17.3 (95 %)	2.5	301.2±5.0	
		Grey subaphiric (snd, cpx) trachytic pumice	G02	K-Feldspar	120.2±12.6 (2σ)	1.4	–	–	97.4±33.8 (95 %)	2.4	302.1±6.8	
			G03	K-Feldspar	124.3±6.4 (2σ)	1.7	–	–	118.2±16.4 (95 %)	2.3	300.3±10.8	
			G02+ G03	K-Feldspar	123.6±6.0 (2σ)	1.4	–	–	115.2±12.8 (95 %)	2.4	301.2±5.2	
Mt. Melbourne surrounding plain	Shield Nunatak	Black lava with olivine and plagioclase	G46	Whole rock	–	–	430.5±82.0 (2σ)	1.1	191±199 (2σ)	0.8	301.2±4.0	Kreutzer 1988: Lower mugearite lava 1.55± 0.05, Upper alkali basalt 0.07±0.05, Armienti et al. 1991: 0.48±0.24
	Markam Island	Black lava with olivine and plagioclase	G49	Feldspar	–		Min=415±24 (2σ)	–	263.0±111.7 (95 %)	5.3	349.7±20.8	
Random Hills (Local Suite)	Harrows Peak	Black lava with olivine and plagioclase	G83	Whole rock	–	–	744.7±66.2 (95 %)	1.8	669±101 (95 %)	1.7	301.2±4.6	
	Pinkard Table	Bomb of vesicular black lava with plagioclase	G26	Whole rock	–	–	1,368±90 (2σ)	1.4	1,307±112 (95 %)	1.4	309.6±15.3	

Wörner and Orsi (1990) as a near-vent strombolian to subplinian pumice fall deposit associated with fluvial to debris flow reworked deposits. We did not observe depositional features that can be reconciled with a fallout origin for the EPI ignimbrite nor extensive reworked material; rather, the unit displays massive, chaotic, polymictic, and poorly sorted facies that are characteristic of deposits from pyroclastic density currents. Furthermore, the high proportion of ash within the ignimbrite (40–70 %), associated with the presence of a co-ignimbrite breccia containing syenite accessory lithics, and the gradational upward compositional zonation from white to black pumice are all characteristic features of Plinian-scale, caldera-forming eruptions, rather than small scale eruptions (e.g. Cas and Wright 1987; Branney and Kokelaar 2002).

Adelie Penguin Rookery lava field Along the southern headland of Edmonson Point, the EPI ignimbrite is intruded by a series of dykes, which can be mapped into the overlying Adelie Penguin Rookery lava field (ARL) that they fed (Figs. 2 and 3a). At Edmonson Point S, the minimum lava thickness in outcrop is 300 m. At Edmonson Point N, the base of the lava field is not exposed, and the thickness in outcrop reaches 550 m. Feeder dykes generally trend N010° to N040° and are 1–10 m thick. Dykes also cross-cut lava units, indicating that the ARL lavas were emplaced during several pulses. Dykes are grey and microcrystalline in the core and show black glassy margins. The lavas are glassy and very fragile and generally show radial columnar jointing, which defines megapillows and tubes associated with breccia domains. These features suggest a sub-aqueous environment, although unequivocal hyaloclastite was not observed. Individual lava units vary from coherent to vesicular and show both basal and top aa-type autobreccias, along with local development of ropy surfaces associated with small lobes. Flow-banding, where visible, is convolute. At Edmonson Point S, above 150 m a.s.l., a series of small scoria cones and spatter agglomerates transitional to coherent lavas are present, fed by N125°-trending dykes (Fig. 4b, c). Scoria cones and agglomerates show no evidence of hyaloclastic fragmentation, suggesting a sub-aerial environment of emplacement. The lava is hawaiitic (sample G39; Appendixes 6 and 7), black in colour, porphyritic, and with phenocrysts of plagioclase (52–77 % An) and olivine (53–65 % Fo). The groundmass is glassy with microphenocrystals of andesine (49–50 % An) and an overall anisotropic texture. At some locations, the lava encloses thermally altered and saccharoidal xenoliths, up to 60 cm

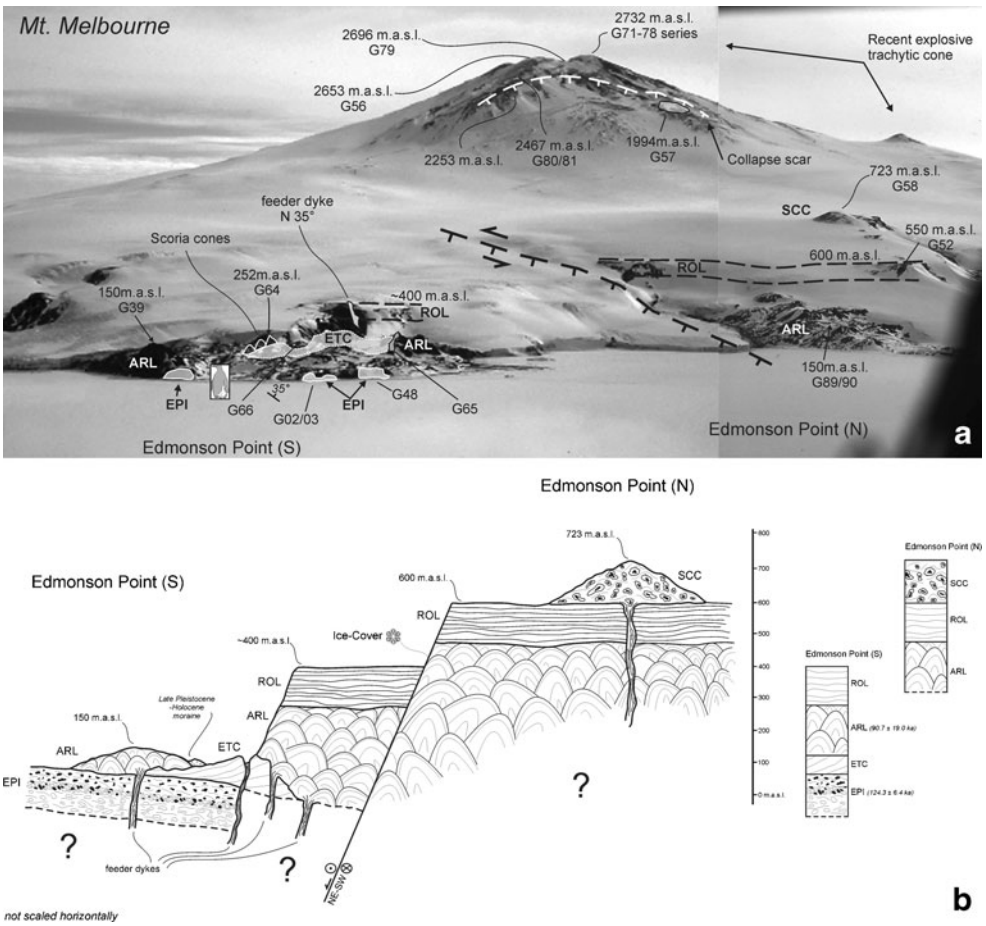

Fig. 2 **a** Helicopter view of the Mt. Melbourne stratovolcano; samples localities (G numbers) and related elevations a.s.l. are indicate; note, below the Mt. Melbourne summit and the presence of a well preserved collapse scar (*white dashed line*) [legend (see text for descriptions): *EPI* Edmonson Point trachytic ignimbrite (123.6±6.0 ka); *ARL* Adelie Penguin Rookery hawaiitic lava field (90.7±19.0 ka); *ETC* Edmonson Tuff Cone; *ROL* 600 m a.s.l. ropey basaltic lava plateau (*black dashed lines* indicate the thickness and exposed extent of the plateau); *SCC* 723 m a.s.l. hawaiite scoria cone]. **b** schematic stratigraphic cross-section of the lower deposits of the Mt. Melbourne stratovolcano at Edmonson Point (see text for explanation)

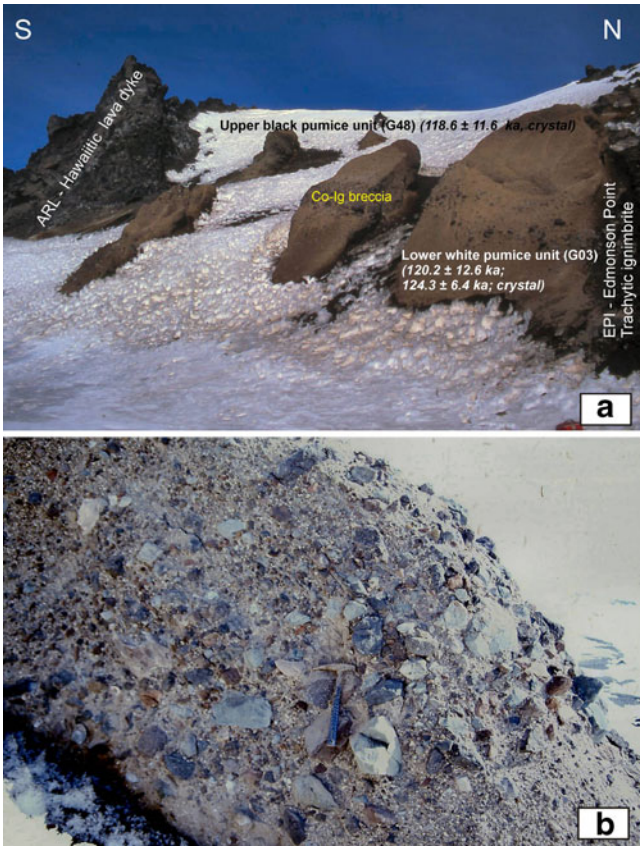

Fig. 3 **a** The "Edmonson Point trachytic ignimbrite" (EPI), cut by a feeder dyke to the "Adelie Penguin Roockery lava field" (ARL); sample numbers and age determinations are reported in brackets (in this and successive figures). **b** detail of the co-ignimbrite breccia lens embedded within the EPI ignimbrite

Fig. 4 **a** The upper part of the ARL lava field is composed of coalescing scoria cones fed by N125°-trending dykes cutting the "Edmonson Point Tuff Cone" ETC. **b** The "Edmonson Point Tuff Cone" (ETC) is composed of stratified lapilli tuff beds; the succession is cut by several small faults

in diameter. Limited outcrops of benmoreitic (sample G40; Appendixes 6 and 7) and trachytic lava units (sample G66; Appendix 6), pale in colour, with a low porphiricity index, were also sampled (cf. Wörner et al. 1989). The phenocrysts include plagioclase (33–39 % An), anorthoclase and sanidine feldspars (52–75 %) Ab, Fe-olivine (30–32 % Fo) clinopyroxenes with exsolution lamellae and resorption sags. The groundmass is holocrystalline with a trachytic texture and the same mineral assemblage.

Edmonson Point Tuff Cone On the southern promontory (Edmonson Point S), there is a lapilli tuff cone sequence covered by the ARL lava and intruded by several about N010°- and N125°-trending ARL feeder dykes (Fig. 4a). The Edmonson Point Tuff Cone (ETC) succession is composed of alternating, moderately sorted, decimetre-thick beds containing monogenetic black lava lapilli and bombs with minor palagonitised coarse ash matrix, and yellow to grey, plane parallel to low-angle cross-stratified, palagonitised, centimetre-thick coarse ash layers (Fig. 4b). The black lava lapilli and bombs are generally equant and glassy, with polygonal geometries that suggest possible moderate interaction with water. Many bombs are bread-crusted and some are spatter-like, occasionally with cores of thermally altered granitoid rocks enveloped in a dark red film of scoriaceous, plagioclase-phyric lava. Such xenoliths are identical to those described for the ARL lavas. No other types of xenoliths were observed, suggesting a very shallow level of magma fragmentation. Rarely, some of the largest bombs form impact sags on the ash layers, indicating a fall component to the deposit, although the presence of low-angle cross-bedding and moderate sorting suggest lateral flow. The ETC, exposed in cliff faces, is cut by normal faults of a few decimetres to 2 m displacement (Fig. 4b). The ETC deposits have been previously interpreted as part of a complex, multiple pumice tuff ring (Wörner and Viereck 1989; Wörner and Orsi 1990). We were unable to locate any juvenile clasts that could be described as pumice clasts, nor any internal unconformity that might indicate multiple sources. We interpret the ETC as a local tuff cone sequence and a member of the ARL lava field. The cone likely formed as a result of local magma–water interaction. It must be

noted that there are no exposures indicative of the stratigraphic relationship between ETC and the EPI ignimbrite, both of which are cross-cut and also covered by the ARL lavas (Fig. 2b). However, the ETC juveniles are identical in composition to the nearby ARL hawaiitic lavas, and the inferred monogenetic style is consistent with the emplacement of the several small lava flows and scoria cones described for the ARL. The stratigraphic position of the ETC member could therefore be at the base of the ARL Formation, or alternatively, within it. We interpret the ARL and ETC units as parts of a small volcanic field (Fig. 2b), where several eruption points were generated along N010°- and N125°-trending feeder dykes. These orientations are consistent with known regional structural trends (e.g. Rossetti et al. 2000) and with the local faults, suggesting a tectonic control over the volcanism in this area. This small volcanic field was emplaced in several pulses, as indicated by the different occurrences of mega-pillows, tuff and scoria cones, produced as a result of different degrees and efficiencies of interaction with water, most likely a melting ice cover (cf. Wörner and Orsi 1990). Given the proximity to the seashoreline and known regional uplift rates (see Fitzgerald et al. 1987), emplacement under sub-aqueous conditions cannot be entirely ruled out, at least for the lowest outcrops of Edmonson Point.

600 m a.s.l. "Ropy basaltic lava plateau" The ARL lava and scoria is covered by a >50-m thick succession of thin, sub-horizontal, alkali-basaltic lava flow units, with interbedded coarse breccia layers, mostly autobreccias. The top of these basalts forms a distinct plateau at about 600 m a.s.l. at Edmonson Point N and at 400 m a.s.l. above Edmonson Point S (Fig. 2). The topmost flow is characterised by perfectly preserved ropey structures, which indicate a subaerial environment. The lava (sample G52; Appendixes 6 and 7) is scoriaceous and porphyritic, with phenocrysts of calcic plagioclase (56–81 % An), Mg-olivine (72–75 % Fo), amphibole (ferro-edenite), ilmenite and magnetite. The groundmass contains fine-grained labradorite, ferro-edenitic amphibole (with composition similar to phenocrysts), clinopyroxene and olivine. Rare gabbroic intraclasts were also observed. The actual contact with the underlying ARL lavas was not observed. We believe, however, that it is a low-relief erosional unconformity because the "Ropy basaltic lava plateau" (ROL) shows an almost constant thickness and a widespread flat top, suggesting that the underlying topography, i.e. the top of ARL, was essentially flat at the time of ROL emplacement. This is somewhat counter-intuitive, considering that the ARL was emplaced from multiple lava sources, scoria cones and spatter agglomerates, and should form a hummocky topography. The ROL plateau shows two distinct elevations, at 400 m a.s.l. above Edmonson Point S and at 600 m a.s.l. above Edmonson Point N, with the difference suggesting displacement by a fault, running NE–SW along the Edmonson glacier tongue valley (Fig. 2). The ROL plateau was described by Wörner and Viereck (1989), who interpreted the lava plateau as having a distal source, although no evidence for this interpretation was provided. We have no evidence for either a local or a distal source for the ROL. The presence of a vertical dyke, feeder to one of the thin lava flows just above Edmonson Point S (Fig. 2b), may, however, suggest a local source to the lava field.

723 m a.s.l. hawaiite scoria cone Above the ROL plateau, an undissected scoria cone rises to an elevation of 723 m a.s.l. (Fig. 2). The cone is composed of quaquaversally dipping, small lava flows (20–30 m thick and lensoidal) interlayered with scoria lapilli and bomb beds. The summit of the cone comprises spatter rags and splinters, and scoria bombs and lapilli (sample G58; Appendixes 6 and 7). Clasts in this unit are moderately porphyritic (5 %), with phenocrysts of Mg-olivine (59–66 % Fo), plagioclase (58–65 % An), clinopyroxene (10 % Wo, 81 % En and 9 % Fs) and amphibole (ferro-edenite–kaersutite). The clasts' groundmass includes fine-grained andesine, amphibole and olivine, with same composition as the phenocrysts. Intraclasts of olivine-gabbro have been identified with plagioclase and Mg-olivine. Many bombs have cores of thermally altered granitoid clasts from the underlying basement.

Summit area

The summit cone of the Mt. Melbourne volcano was surveyed, from the summit crater (2,732 m a.s.l., Fig. 5a) down to 2,253 m a.s.l. (Fig. 2). The area was described previously in Wörner and Viereck (1989, 1990). The crater rim is uniformly covered by a blanket (10–70-cm thick) of dark grey juvenile lapilli and bombs up to 50 cm in diametre (Fig. 5c, d) and a variety of xenolith blocks, which include variably porphyritic, massive to flow-banded, pale grey to dark lava and clasts of older pyroclastic material, as well as pre-volcanic rocks. The blanket is a fall deposit and probably from the most recent eruption. The juvenile products (samples G56, G57 and G75; Appendixes 6 and 7) are mainly trachytic to rhyolitic, grey, porphyritic, vesicular to dense clasts, with some showing spatter morphology and internal rheomorphic textures produced by post-fragmentation ductile deformation (Fig. 5c). Phenocrysts include plagioclase (20–38 % An), and clinopyroxene (44–46 % Wo, 18–23 % En and 30–36 % Fs) and Fe-olivine (13–16 % Fo), whereas the groundmass contains Na-sanidine, clinopyroxene, plagioclase, opaques and F-apatite crystals. The deposit also contains dense clasts of trachyte and rhyolite, which may be either dense juvenile clasts or xenoliths

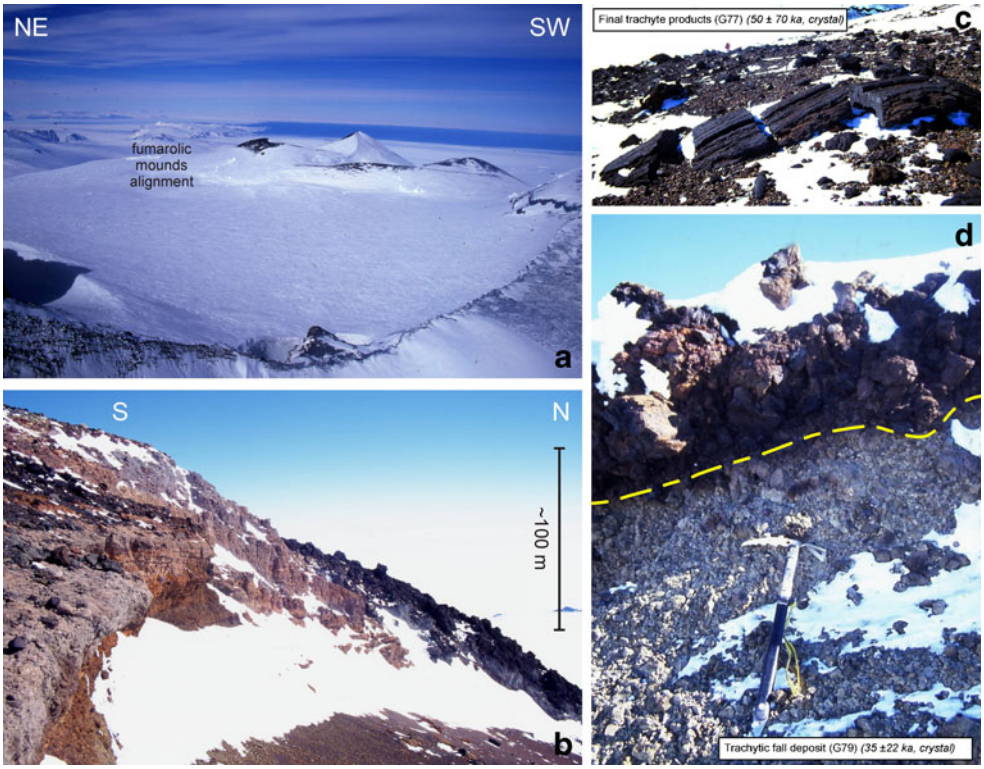

Fig. 5 **a** The summit crater floor (ca. 600 m in diametre). **b** the eastern flank of the volcano is cut by an arcuate vertical scarp (see also Fig. 2), several tens of metres high, which shows hydrothermally altered pyroclastic rocks (note the pale colour); this scar is interpreted as an incipient sector collapse. **c** The uppermost tephra which blanket the summit crater rim are trachytic scoria and spatter bombs, which cover conformably (**d**) grey, trachytic pumice lapilli and bomb bed up to 15 m thick. Note the coarsening upward grain size

from older lavas (samples G73, G77, G78 and G80). One sample (G71; Appendixes 6 and 7) from the crater rim is a black, porphyritic, vesicular lava bomb containing phenocrysts of calcic-plagioclase (59–66 % An), Mg-olivine (65–75 % Fo) and clinopyroxene (47 % Wo, 37 % En and 16 % Fs), and rare ferro-richterite amphibole set in a groundmass of calcic plagioclase and olivine. Accessory lithics of gabbroic–dioritic composition are also present.

The upper coarse fall deposit covers gradationally a lower pumice lapilli unit, more than 15-m thick and exposed inside the northern crater wall (Fig. 5d). This deposit is clast-supported, ash-matrix-free, sorted and composed largely of angular pumice clasts (average of 4–5 cm in diametre, with blocks up to 20 cm large), locally broken in-place into smaller, jigsaw-fit pieces. These characteristics are consistent with pyroclastic fall origin. The pumice (sample G79; Appendixes 6 and 7) is pale grey, highly vesicular, porphyritic with phenocrysts of anorthoclase (63–68 % Ab) and clinopyroxene (32–52 % Wo, 6–8 % En and 41–60 % Fs); anorthoclase glomerocrysts (63–64 % Ab) are also present.

At 2,253 m a.s.l. (N74°21′10.9″; E164°44′47.6″) is a subvertical cliff about 50–100 m high (Figs. 2 and 5b), which exposed hydrothermally altered (yellow to red in colour) pyroclastic deposits, cut by several N–S oriented open fractures. This cliff can be traced across the entire eastern flank of the volcano, with a N–S orientation, forming a clear arcuate, down-slope concave structure (Fig. 2). We infer that the cliff corresponds to a previously unidentified incipient collapse scar and also represents a zone of recent, focussed hydrothermal activity that is not evident elsewhere along the volcano slopes.

Dispersal of the most recent fall deposits

Where seracs cut through the ice cover of the Mt. Melbourne stratocone, continuous layers of tephra are seen (Fig. 6a), as previously described by Lyon (1986). We sampled the topmost tephra layer, 16 km NE of the summit (Figs. 1 and 6c; sample G62). The tephra occurs just 10 cm below the ice top and is consistently 3-cm thick, and is composed of well sorted, pale grey, highly vesicular (>60 %) and poorly porphyritic angular trachytic pumice 1.5 cm lapilli, with maximum size of 2 cm (Fig. 6d). The deposit contains 1 % of 0.5 cm lava lithic clasts (Fig. 6d). There are phenocrysts of plagioclase (21 % An), Fe-olivine (15 % Fo) and clinopyroxene (46 % Wo, 21 % En and 33 % Fs). The depositional characteristics are typical of a primary fall deposit. Characteristics such as the texture of the pumice, the composition of mineral phases and the bulk trachytic composition (Appendixes 6 and 7; Appendix 8 also reports trace elements data) are all consistent with those of the most recent deposit at the summit crater (sample G56), which we infer correlative. Other apparently correlative deposits

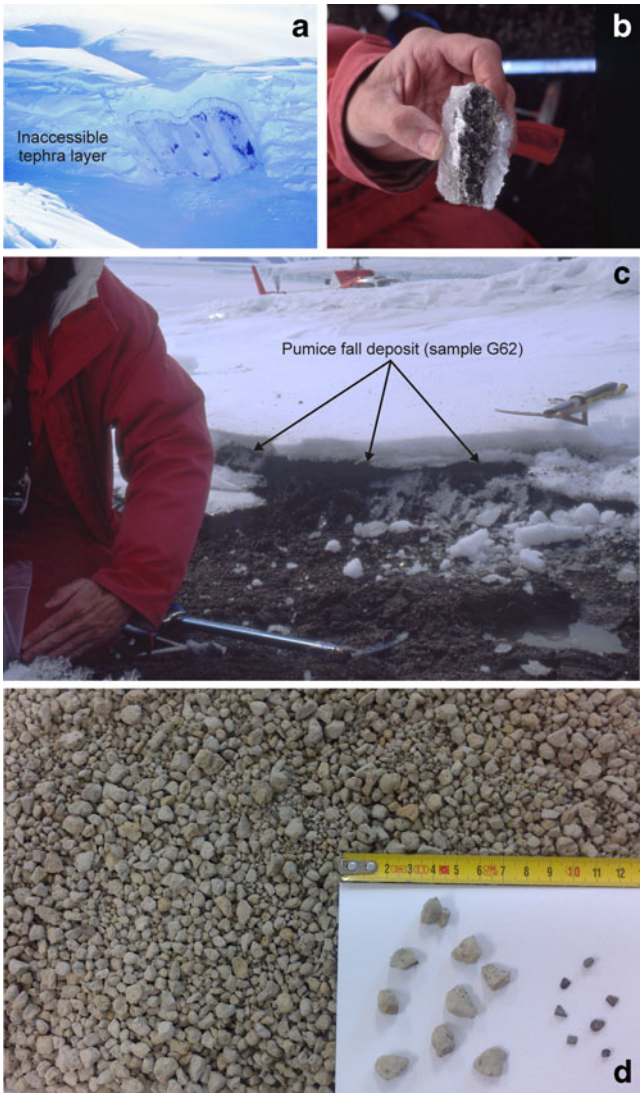

Fig. 6 **a** Helicopter view of ice-seracs (approximate cliff's height 100 m), which show continuous layers of ash of likely fallout origin. **b** Sample G62 is composed of a 3-cm-thick pumice lapilli layer embedded in ice near Baker Rocks, 16 km to the NNE of the Mt. Melbourne summit. **c** The outcrop area for sample G62. **d** Grainsize of pumice and lithic clasts of G62; clasts in the *lower white inset* are the largest

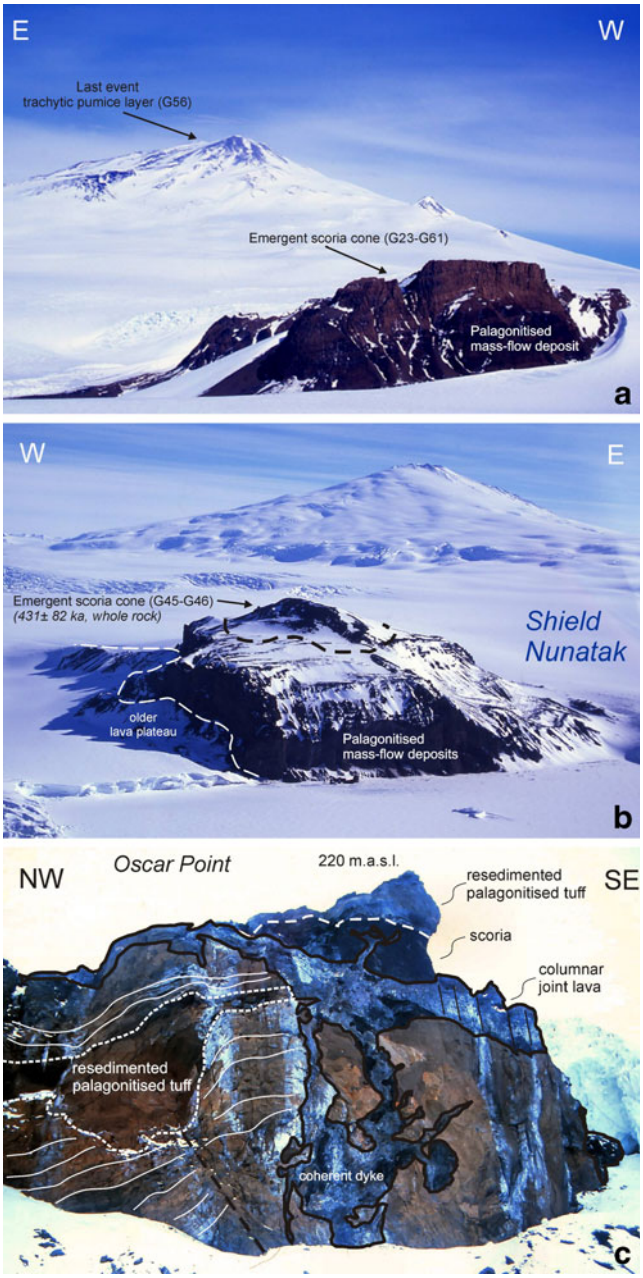

Fig. 7 Helicopter views of monogenetic centres peripheral to Mt. Melbourne: **a** Baker Rocks, **b** Shield Nunatak, **c** Oscar Point: a >200 m thick succession of thinly bedded palagonitised lapilli tuffs is cut by several wavy dikes and apophyses, which are feeders to a summit scoria cone deposit

exposed along vertical cliffs (Fig. 6a) east and west of the summit are inaccessible, so we could not produce an isopach map of this fall deposit.

Mt. Melbourne peripheral centres

Approximately 10–25 km from the Mt. Melbourne summit are several monogenetic volcanic centres. The most prominent are Baker Rocks in the northern area (Fig. 7a), and Shield Nunatak (Fig. 7b), Oscar Point and Markham Island in the southern area (Fig. 7c). North of Baker Rocks, a series of similar but smaller monogenetic volcanoes, outcrop along the coastal cliffs (N74°12′34.7″; E164°48′22.0″ and N74° 09′02.9″; E164°47′26.2″) up to 400 m a.s.l. (N74°19′031″; E165°03′002″). Shield Nunatak has been described in detail by Wörner and Viereck (1989). The main characteristic common to Baker Rocks, Shield Nunatak and the cliffs immediately to the west of Oscar Point is a yellow to orange, lower succession 50–300-m thick of palagonitised lapilli tuffs, cut through by wavy dikes and apophyses that are feeders to scoria cones and lava flows (Fig. 7c). The

palagonitised lapilli tuffs are also cut by unconformities, and syn-eruptive faults and fractures, and show extensive soft-sediment deformation. The lapilli tuffs are ubiquitously bedded, alternating poorly sorted, centimetre-thick ash layers and moderately sorted, decimetre-thick lapilli beds. Beds locally show both normal and inverse grading. Armored lapilli are common. Lapilli-sized clasts are dense to vesicular dark and glassy lava, generally polygonal in shape. This suggests that the clasts are juvenile fragments from hyaloclastic/phreatomagmatic processes of fragmentation (Cas 1992; McPhie et al. 1993). Bedding varies from parallel- to low-angle cross-stratified, which suggests emplacement by variably concentrated density currents. Generally, no lithics from the underlying basement were found. These features together are interpreted to indicate monogenetic eruptions in a sub-glacial (or sub-aqueous) environment. Once the ice cover melted completely (or the thickness of the deposit exceeded the water depth), phreatomagmatic and hyaloclastic fragmentation ceased, giving way to strombolian to effusive eruptions (e.g. Wörner and Viereck 1989; Smellie and Chapman 2002 and references therein).

The scoria and lava that form the sub-aerial scoria cone at the top of Shield Nunatak are porphyritic alkali basalt (samples G45 and G46; Appendix 6), with phenocrysts of augitic clinopyroxene, olivine (70–80 % Fo) and plagioclase (56–64 % An), set in a groundmass of labradoritic plagioclase (52–56 % An), clinopyroxene and olivine similar in composition to phenocrysts. Alkali-basaltic rocks erupted from Shield Nunatak have textures, phenocrysts assemblages and groundmass associations very similar to those of Markham Island (sample G49), Oscar Point (sample G50) and Baker Rocks (samples G23 and G61)(Appendixes 6 and 7).

The monogenetic volcanic field distributed across the Transantarctic Mountains

The Random Hills area is located north of Mt. Melbourne (Fig. 1) and comprises a series of monogenetic scoria and lava centres, directly overlying the Ordovician granitic basement. In the Random Hills area, *Pinkard Table* is a NNE–SSW ridge, topped by a series of small, perfectly preserved, scoria cones (Fig. 8a), not previously described. The scoria cones are at ~1,600 m a.s.l. and are composed of lapilli and bombs, with the latter including highly vesicular scoria and subordinate lava fragments and xenoliths derived from the underlying granite basement. Scoria clasts are red, with some plastically deformed. The scoria is a highly porphyritic alkali basalt (sample G26; Appendix 6) with calcic-plagioclase (labradoritic), relics of altered forsteritic olivine, diopsidic clinopyroxene, microphenocrysts of edenitic amphibole and ilmenite as the dominant phenocrysts phases. The groundmass is microcrystalline labradoritic plagioclase. The geometry and structure of the scoria cones, as well as the absence of any indication of magma–water interaction, suggests that the style of activity was strombolian and the environment sub-aerial. A few kilometres to the east of Pinkard Table, four well-preserved small scoria cones, are perfectly aligned along the N–S crest (Fig. 1). The scoria products of these cones are hawaiitic in composition (sample G38; Appendix 6) with similar petrographic characteristics to that of the Pinkard Table centre.

Further to the east, the *Harrow Peaks* outcrop is located on a saddle at 800 m a.s.l. (Wörner and Viereck 1989) and characterised by an eroded centre composed of a prominent black porphyritic lava plug, with megapillow structures up to 40 m across (Fig. 8c). The plug is fed by a N008°-oriented dyke, which intrudes one of the many parallel fractures that pervasively cut the Ordovician granite basement. The lava plug is in transitional to intrusive contact with palagonitised yellow to brown lapilli tuffs (Fig. 8d), which generally dip (20°) almost parallel to the present day steep slopes of the saddle, down to 300 m a.s.l. The lower beds of the palagonitised tuff include many blocks of the underlying granite, some of which are rounded. The lava is a hawaiite (sample G83; Appendix 6), with sparse phenocrysts of clinopyroxene (augite–Fe–augite) and plagioclase (40–44 % An) and accessory magnetite in a microcrystalline groundmass. Previously undescribed monogenetic centres, showing petrographic, stratigraphic and morphologic characterstics very similar to Harrow Peaks, occur to the south (N74°06′44.3″; E164°45′32.9″; 449 m a.s.l.), and further north, along the Tinker Glacier valley (N74°56′40.5″; E164°25′49.7″; 353 m a.s.l.).

To the southwest of Mt. Melbourne, small monogenetic centres are scattered on the Deep Freeze Range, Browning Pass and the Northern Foothills, including the small, previously undescribed scoria cone of Mt. Abbott (Fig. 8b), just west of the Italian Base (Fig. 1). Mt. Abbott scoria cone is well preserved and is composed of loose, reddish to brown scoria bombs and lapilli, and spatter bombs. Sample G25 (Appendix 6) from this locality is an alkali basaltic with andesinic plagioclase.

Geochronology

Twenty-six sites from the Mt. Melbourne area were initially sampled for $^{40}Ar/^{39}Ar$ age determinations (Appendix 1). Unfortunately, due to younger than expected ages and low potassium concentrations, insufficient feldspar was recovered from a number of samples. Consequently, $^{40}Ar/^{39}Ar$ results are reported for only seven feldspar separates (Table 1). Based on initial feldspar age results, five additional, holocrystalline lava samples were selected for whole-rock $^{40}Ar/^{39}Ar$ step-heating analyses (Table 1). Analytical metods are detailed in Appendix 2.

$^{40}Ar/^{39}Ar$ results obtained from seven feldspar separates and five whole-rock samples are summarised in Table 1 and

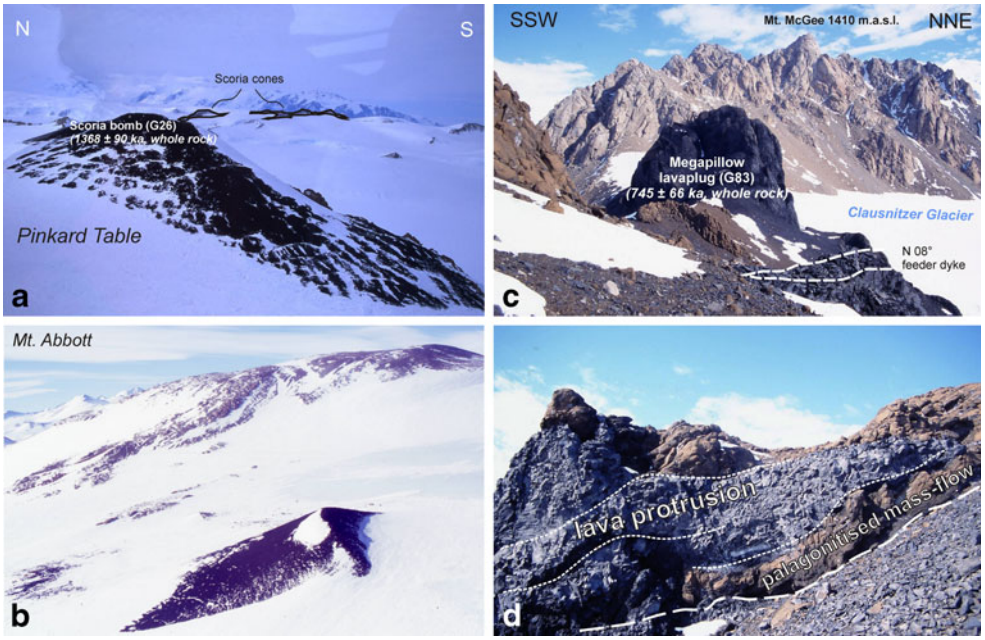

Fig. 8 **a** One of the preserved scoria cones at the top of the Pinkard Table crest (1,600 m a.s.l.). **b** Helicopter view of Mt. Abbott (529 m a.s.l.). **c** Helicopter view of the Harrow Peak centre; the main outcrop is a 30-m high lava plug, with radial jointing. **d** The main lava plug laterally feeds small lava intrusions cutting the associated palagonitised hyaloclastitic debris

Fig. 9. Detailed analytical data are listed in Appendixes 3 and 4. All uncertainties are reported at the 95 % confidence level. The volcanic successions at Edmonson Point yielded age results of variable uncertainty. The lowermost EPI ignimbrite (Figs. 2 and 3) produced the most consistent ages, from three different samples (G02, G03 and G48). Samples G02 and G03 yielded plateau ages of 120.2±12.6 and 124.3±6.4 ka, respectively. Isochron ages are within error of these ages, with $(^{40}Ar/^{36}Ar)_i$ ratios indistinguishable from the atmospheric value of 295.5 (Table 1). The weighted mean age for all plateau segments from G02 and G03 is 123.6±6.0 ka. Although sample G48 did not produce a statistical plateau age, all steps have broadly similar ages, averaging 118.6±11.6 ka (Table 1). The consistency of the above results provides confidence in the about 120 ka age for this unit. The overlying ARL lavas produced more discordant ages. Three whole-rock aliquots of sample G39 yielded statistical plateau ages, but with large uncertainties. The weighted mean age for the three aliquots is 298±55 ka. However, isochron plots for this sample produced a negative age result and an elevated $(^{40}Ar/^{36}Ar)_i$ ratio, possibly indicating some excess argon contamination (Table 1). In contrast, K-feldspar from sample G66 gave a plateau age of 90.7±19.0 ka, with a similar isochron age and atmospheric $(^{40}Ar/^{36}Ar)_i$ ratio (Table 1). Supported by stratigraphic relationships, we suggest that the latter age of about 90 ka provides the best estimate for the age of ARL lava field. Only one sample (G52) was dated from the ROL alkali-basaltic ropy lavas, which overlie the ARL lavas. Three whole-rock aliquots from sample G52 again produced plateau ages, but with large uncertainties, giving an imprecise weighted mean age of 112±84 ka (Table 1). This age is within error of results from the underlying lavas and, within the uncertainties, is also consistent with stratigraphic relationships. G77 and G79 represent samples of the youngest volcanic deposits on Mt. Melbourne. Feldspar separates from both samples released very low quantities of radiogenic ^{40}Ar, resulting in very imprecise plateau ages of 50±70 and 35±22 ka, respectively (Table 1). These data suggest an Upper Pleistocene to Holocene age for these deposits. In addition, a grey pumice lapilli fall deposit, very similar in chemistry to G56 and G77 (see Appendix 6), occurs in the upper ice cap in the area (sample G62; Fig. 6c), supporting a very young age. In addition to the Mt. Melbourne volcanic samples, $^{40}Ar/^{39}Ar$ results were also obtained from volcanic deposits in the area surrounding Mt. Melbourne. Three whole-rock lava aliquots of sample G26, from Pinkard Table, yielded plateau ages, with a mean age of 1,368±90 ka (Table 1). Similar whole-rock aliquots from a Harrow Peaks (Random Hills) lava sample (G83) are characterised by a mean age of 745±66 ka (Table 1). Whole-rock aliquots from a Shield Nunatak lava sample (G46) produced more discordant results, with an imprecise average age of 431±82 ka (Table 1). A final plagioclase feldspar sample from Markham Island (G49) yielded a discordant age spectrum, with a maximum apparent age of 415±24 ka, an imprecise isochron age of 263±112 ka and an $(^{40}Ar/^{36}Ar)$ ratio of 350±21 (Table 1). These results only constrain these Markham Island volcanic deposits to be less than ~400 ka.

Whole-rock geochemistry

A total of 31 sites from the Mt. Melbourne area were sampled for geochemical analysis (Appendix 1). Analytical methods are detailed in Appendix 2.

The major elements for the analysed samples are presented in Appendix 6 and used to classify the volcanic rocks

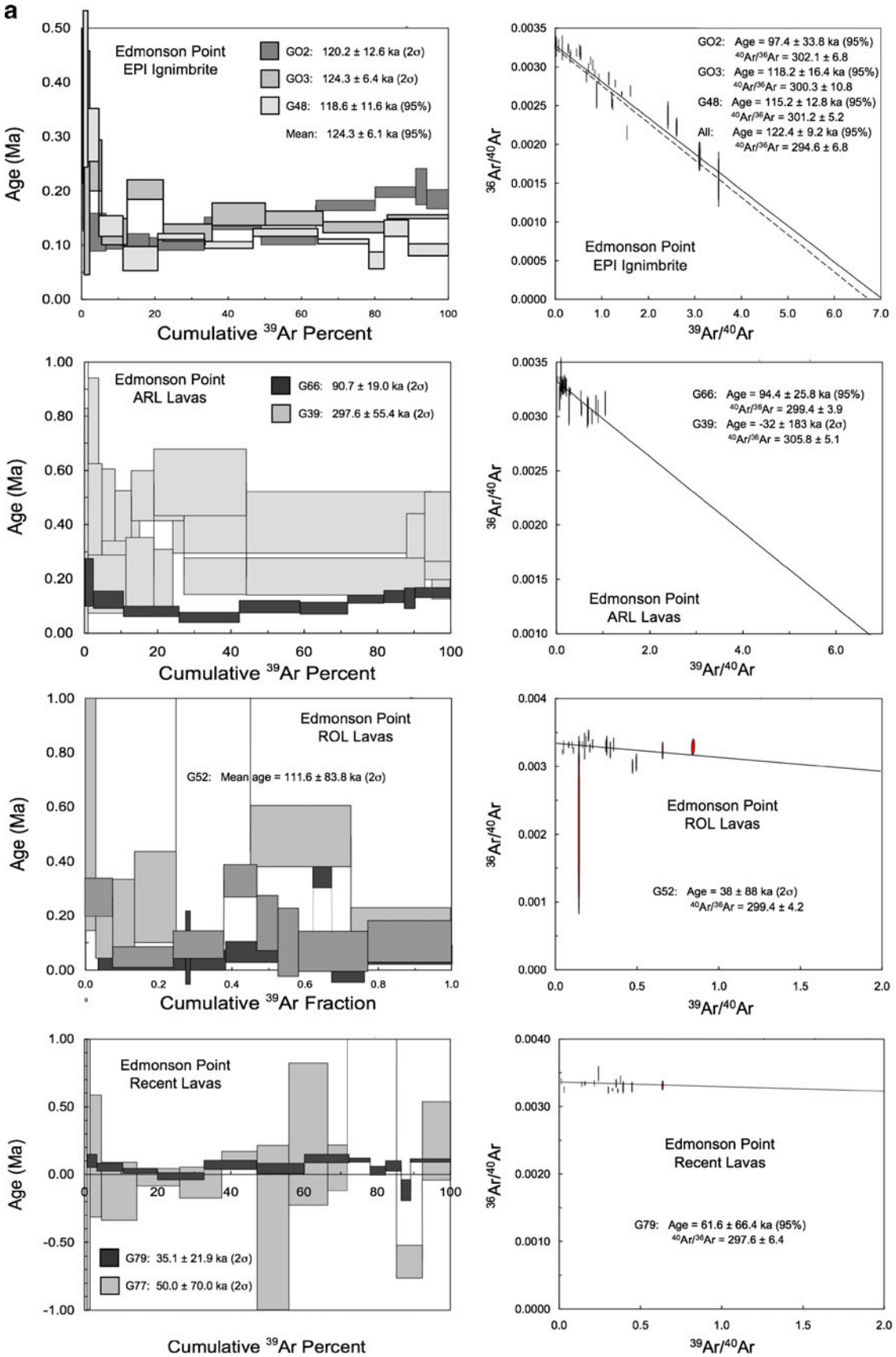

Fig. 9 Plateau ages (box heights are 1σ) and $^{36}Ar/^{40}Ar$ *vs* $^{40}Ar/^{39}Ar$ plots for the dated samples (data-point error ellipses are 68.3 % confidence)

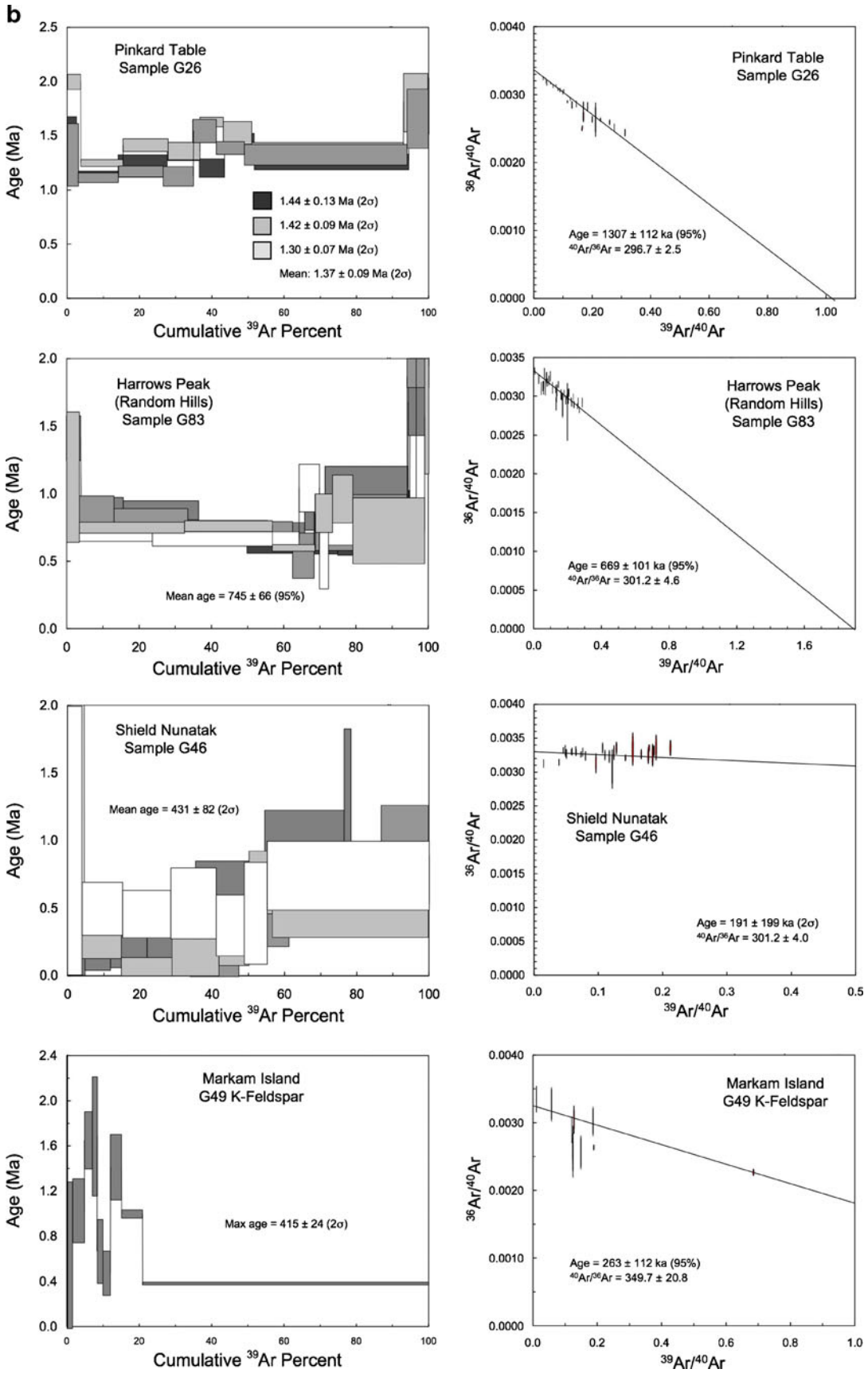

Fig. 9 (continued)

according to LeMaitre (2002). A complete discussion of the geochemistry data, including trace elements, is beyond the scope of this paper, which is centered on the stratigraphy and geochronology of Mt. Melbourne. Analyses were recalculated to 100 % on a volatile-free basis and plotted on a total alkali-silica (TAS) diagram (Fig. 10a). CIPW norms and Alkali Index were calculated for all samples to evaluate (1) the normative content of quartz (Q), nepheline (Ne) and leucite (Lc) and hence the variations in silica saturation and (2) the evolution of the $[K_2O/(K_2O+Na_2O)]\times100$ index and the alkali signatures of the magmatism in the area. All the studied samples belong to the alkaline series (Fig. 10a), according to classifications proposed by Kuno (1966), Irvine and Baragar (1971) and Bellieni et al. (1983). The least evolved rocks are alkali basalts. Differentiated products include intermediate hawaiites, benmoreites (based on their sodic signature; Na_2O–2.0>K_2O; LeMaitre 2002) and trachytes (normative equation $[100\times Q/(Q+An+Ab+Or)]$ always<20 %; Le Bas and Streckeisen 1991). Remarkably, benmoreites are rare and mugearitic rocks absent, suggesting the occurrence of a compositional gap, termed the Daly gap (e.g. Bonnefoi et al. 1995) also recognised for other Cenozoic volcanic complexes of Northern Victoria Land (Wörner and Viereck 1989; Armienti and Tripodo 1991; Armienti et al. 1991; Beccaluva et al. 1991a, b; Müller et al. 1991). The most explosive eruptions have been trachytic, such as the one that produced the Edmonson Point Ignimbrite (samples G03 and G48; Appendix 6). Two samples plot in the rhyolite field, close to the boundary with trachytes (Fig. 10), and are from the pyroclastic deposits at the top of Mt. Melbourne (samples G75 and G78; Appendix 6). The rhyolites at Mt. Melbourne had not been reported previously. The presence of normative corundum (0.8 %) in G75 and normative acmite (2.7 %) in G78, together with the Agpaitic Index $[(Na_2O+K_2O)/Al_2O_3$ molar ratio] in the range of 0.94–1.04, do not permit a clear definition of the peralkaline character of these rocks. All analysed samples belong to the Na-Alkaline series, showing a strong Na signature (AI< 35 %; AI=Alkali Index $[K_2O/(K_2O+Na_2O)]\times100$; Stewart and Thornton 1975; D'Amico et al. 1989) for the least evolved rocks, and a low-K signature (40 %<AI<50.7 %) for the benmoreiitic, trachytic and rhyolitic rocks. The progressive K_2O enrichment in evolved rocks (Fig. 10b) reflects the kaersutite–kataphorite amphibole in less evolved products versus Na-sanidine+anorthoclase feldspars in the most evolved samples (Appendix 7a, e). CIPW normative compositions are characterised by the presence of nepheline (Na-foid, 0–4.6 %), with leucite always absent (K-foid, 0 %) and normative quartz <15 % (*Q*, 0–14.6 %) (Appendix 6), highlighting the evolutionary trend from silica-undersaturated (normative nepheline content of 1.4 % at Random Hills, 1.1 % at Markham Island, and 4.6 % at Edmonson Point), to slightly silica-oversaturated conditions (maximum normative quartz content of 14.6 % at Mt. Melbourne summit crater

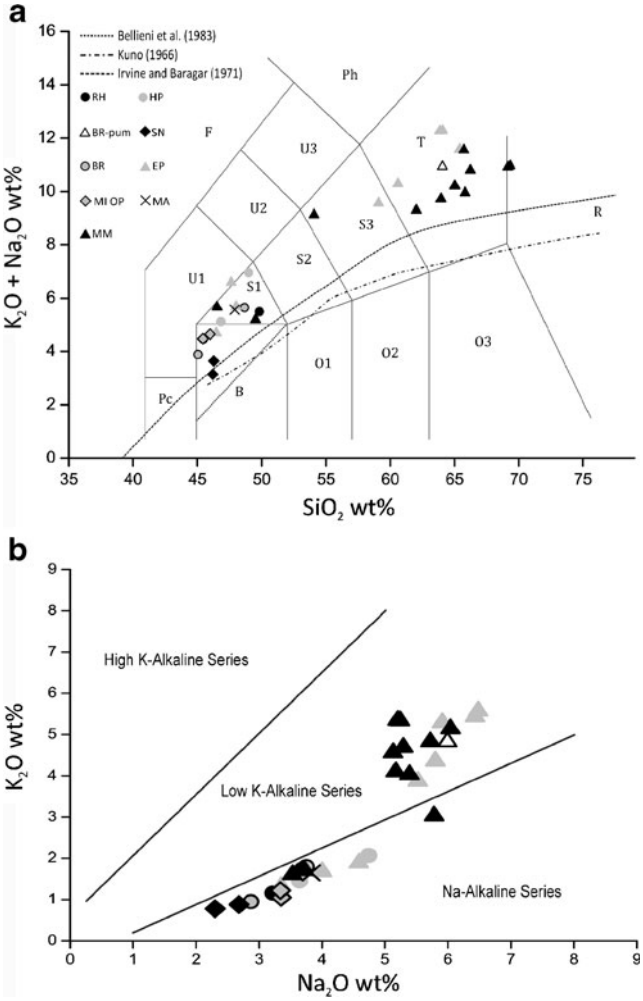

Fig. 10 **a** Total alkali-silica diagram (Le Bas et al 1986; Le Bas and Streckeisen 1991) for samples analysed in this study. *RH* Random Hills, *HP* Harrow Peaks, *BR* Baker Rock, *EP* Edmonson Point, *MM* Mt. Melbourne, *BR* pumice layer G62, *SN* Shield Nunatak, *MI OP* Oscar Point/Markham Island, *CW* Cape Washington, *MA* Mt. Abbott. **b** Classification of the alkali signature of the analysed samples in a K_2O vs. Na_2O wt% diagram

trachytes). The Harker diagrams shown in Fig. 11 illustrate the linear correlation of major oxides vs. SiO_2 (wt%) [see also Appendix 8 for selected LILE and HFSE elements abundances and relative bivariate diagrams vs. SiO_2 (wt%)].

Discussion

This study has generated a new set of stratigraphically linked geochronology and geochemistry data, which were used to develop an improved temporal reconstruction of the Mt. Melbourne volcanic field. However, the presence of extensive ice cover on the volcanic field limits evaluation to scattered outcrops (Figs. 1 and 2), which places limitations on any comprehensive interpretation of the volcano's evolution. Our data

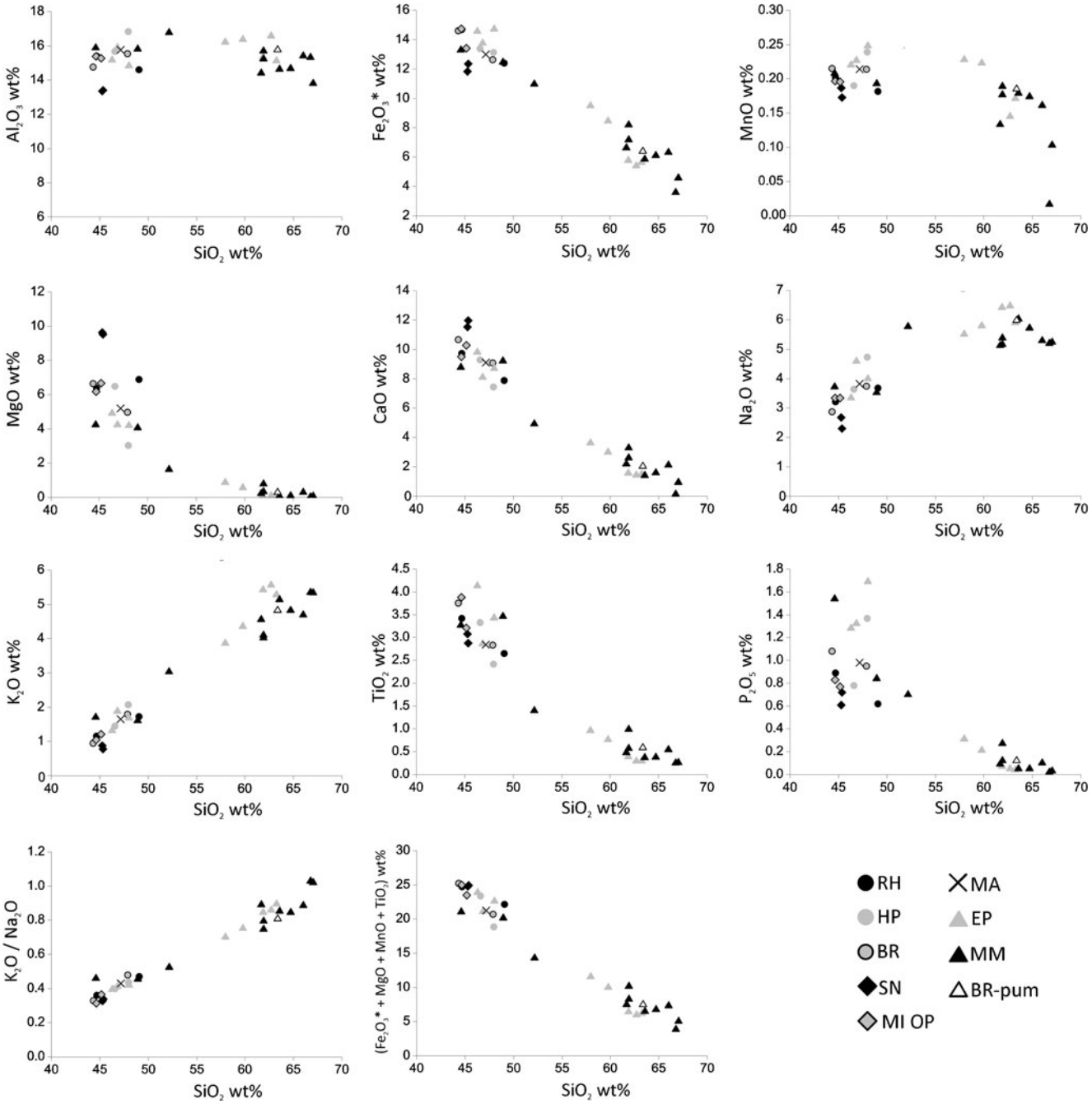

Fig. 11 Harker diagrams for major oxides vs. SiO_2 wt% and total ferromagnesian vs. alkali ratio diagram

cover most of the existing outcrops, however, and provide the best available basis for reconstructing the main events in the evolution of the Mt. Melbourne volcanic field.

Evolution in time and space of the volcanic activity

The only work that has previously attempted to summarise the volcanological evolution of the Mt. Melbourne volcanic field is that of Wörner and Viereck (1989). Lacking a reliable age data set, those authors used the erosional character, inferences of magma–ice interaction, the available ages, and the geographic distribution of magma types, to reconstruct five phases of volcanism: (1) the oldest phase involved the emplacement of the Washington Ridge (2.6–1.7 Ma Kreutzer, 1988, unpublished data) and the Random Hills monogenetic volcanoes, with magmas belonging to a basanite-tephrite trend; (2) trachytic xenoliths found in the Mt. Melbourne pyroclastics were interpreted as belonging to

a pre-Older Drift volcanic phase, possibly as old as 2.5 Ma; (3) the mugearitic lavas at the base of Shield Nunatak (unconstrained age of 1.55 Ma; Kreutzer, 1988, unpublished data), along with volcanic centres of Baker Rocks, Edmonson Point and Oscar Ridge, were interpreted as an "older series", also pre-Older Drift; (4) the emergent sub-glacial to sub-aerial alkali basalts and hawaiites of Shield Nunatak and Oscar Ridge were attributed to a "younger series" of pre-, syn-Younger Drift age; (5) finally, the alkali basalt to trachyte products of Mt. Melbourne were emplaced from an unconstrained age up to recent times. Later K-Ar age determinations by Armienti et al. (1991) indicated a 12–3 Ma age range for the Random Hills monogenetic volcanism, and 0.7–0.4 Ma for Oscar Point and Shield Nunatak, respectively, the latter contrasting with the pre-, syn-Younger Drift age suggested by Wörner and Viereck (1989).

Based on our data, we present a substantially different reconstruction of Mt. Melbourne volcanic field's evolution and suggest that neither the erosional aspect nor the extent of magma-water(ice) interaction can be used successfully in this area to constrain the succession of volcanic phases. This conclusion is based on the following considerations. The first is that Antarctic glaciers have had very different types of erosional behaviours over time and location (e.g. Di Nicola et al. 2009), due to climate changes and local extent of the ice cover; it is therefore difficult in the Mt. Melbourne area to use such an approach. For example, the 1,368 ka scoria cone at Pinkard Table appears almost pristine despite being much older than the 745 ka lava edifice at Harrow Peaks (Fig. 8a, b). It is therefore very difficult to use morphology as an indicator of age. Indication of magma–water (ice) interaction is also not a particularly reliable procedure to establish periods when the ice cover was present. Magma–ice interaction depends on many factors, of which the ice thickness is only one. Furthermore, in Antarctica, glaciers behave very differently depending on whether they are from the continental ice sheet, or represent small local glaciers, as is the case for the Mt. Melbourne area, where the net accumulation and mass balance with time varies locally (Orombelli et al. 1991; Jacobs 1992). Our approach, therefore, is to use only the observed stratigraphic relationships and the associated age determinations, together with chemical compositions to reconstruct the volcanic evolution of the region. The evolution of the Mount Melbourne volcanic field can be described in three main periods, characterised by distinct volcanic systems and different volcanic styles (Fig. 12).

Random Hills Period The new $^{40}Ar/^{39}Ar$ age determinations presented in this paper indicate that the monogenetic centres belonging to the Local Suite (Random Hills and Mt. Abbott) are Lower–Middle Pleistocene, and postdate the emplacement of the Pliocene Cape Washington shield volcano (Fig. 12a, b). Ages obtained at Pinkard Table and at Harrows Peaks are 1,368±90 and 745±66 ka, respectively, but distinctly younger than previous K–Ar determinations (Armienti et al. 1991; Appendix 5). It is well known that the K–Ar dating method has a number of limitations, particularly an inability to reveal argon loss or gain, and various analytical issues. The $^{40}Ar/^{39}Ar$ method largely overcomes these limitations and usually produces more precise and accurate age results. In this case, the older K/Ar dates could be due to the presence of excess argon, analytical issues or even analysis of different volcanic units. As Armienti et al. (1991) provide little description of their samples, sampling localities and analytical methods, it is not possible to further evaluate the reasons for the discrepancies.

The small lava volumes and the poorly evolved, mafic compositions suggest that this dominantly effusive volcanism was associated with lithospheric fractures able to tap small batches of magma from the mantle, as also indicated by the xenoliths in these rocks (cf. Hornig et al. 1991; Beccaluva et al. 1991a, b; Wysoczanski and Gamble 1992). In the Mt. Melbourne area, projection of the main dextral transcurrent Priestly and Campbell fault systems (Fig. 1), which controlled Cenozoic magmatism across this part of the Transantarctic belt (Rossetti et al. 2000; Storti et al. 2006), indicates that active intraplate tectonics may control local extension, the degree of partial melting, and the passage of mantle-derived magma through the crust (Rocchi et al. 2003).

Wörner and Viereck (1989) document a mugearitic lava flow at the base of Shield Nunatak, and report an age of 1.55 Ma (Kreutzer, 1988, unpublished report; Table 1). If the age of this lava flow is correct, then differentiated magma also erupted during the Random Hills Period.

Shield Nunatak Period Closer to Mt. Melbourne, we obtained two imprecise, though consistent, ages for the monogenetic centre of Shield Nunatak (431±82 ka) and Markham Island (<400 ka) (Fig. 12c). Previous published ages for Shield Nunatak are quite discordant, ranging from 0.07±0.05 Ma (Kreutzer, 1988, unpublished report quoted in Wörner and Viereck 1989) to 0.48±0.24 Ma (Armienti et al. 1991). The latter result is consistent with our $^{40}Ar/^{39}Ar$ ages, whereas the younger age of 0.07±0.05 Ma appears anomalous. Possible explanations for the young K-Ar age include analytical issues such as incomplete degassing of argon, a common problem associated with retentive feldspar-rich melts. If our older result is correct, it suggests that, during the Middle Pleistocene, the volcanic activity, which also produced Oscar Point (0.71±0.18 Ma in Armienti et al. 1991; Appendix 5) and Baker Rocks (0.74 ±0.1; 0.2±0.04 Ma in Armstrong 1978; Appendix 5), moved progressively toward the younger centre of volcanic activity associated with Mt. Melbourne. The magma

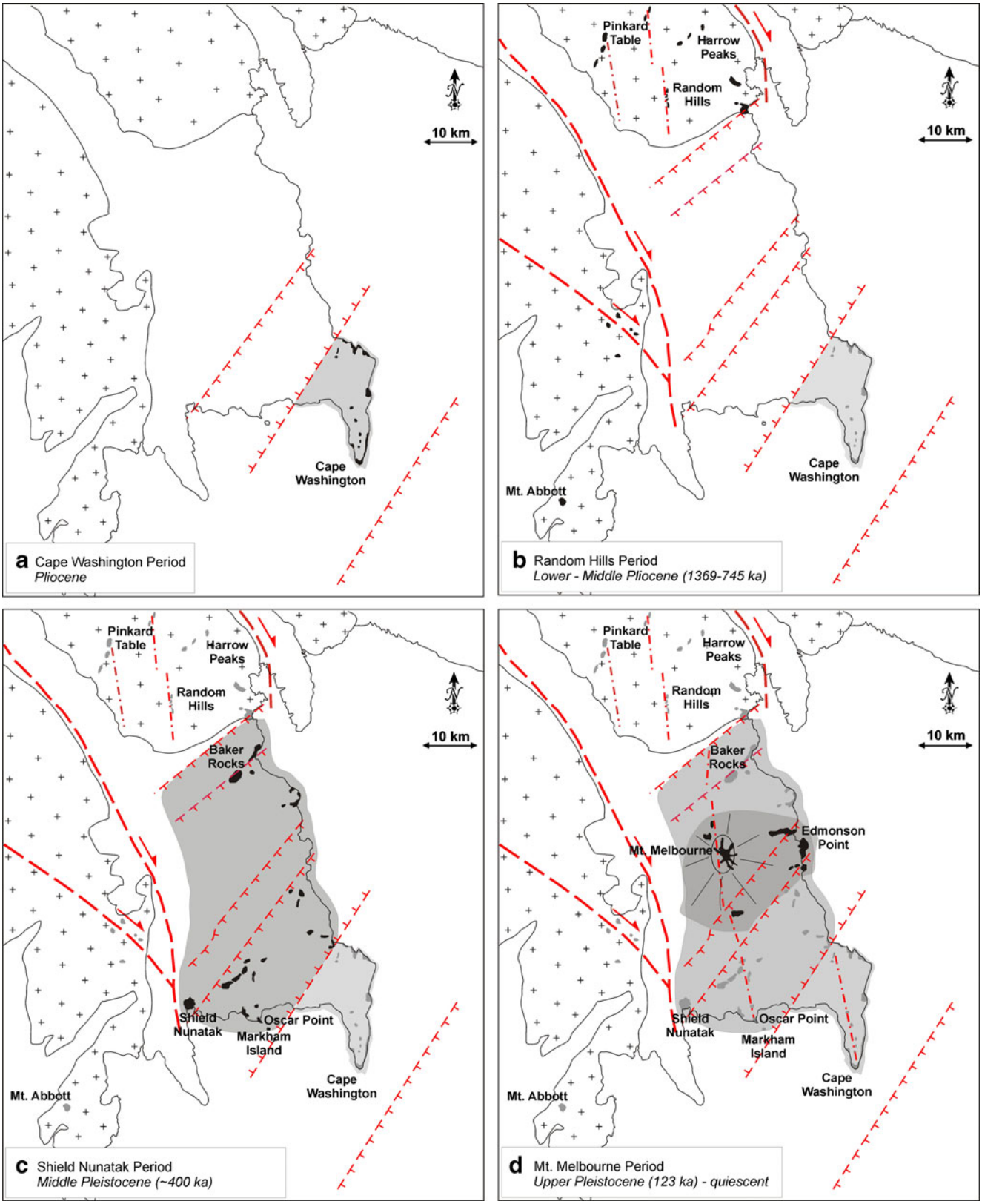

Fig. 12 Evolution of Mt. Melbourne volcanic field (see text for explanation)

chemistry is alkali basaltic for all these centres, indicating continuity with the previous Random Hill Period.

Mt. Melbourne Period (Fig. 12d) The oldest exposed deposit associated with the Mt. Melbourne stratovolcano is the

trachytic EPI ignimbrite at Edmonson Point, dated at 123.6± 6.0 ka. Although the restricted exposure of the EPI ignimbrite limits support for interpretations of the eruption, some can be made. The first is that the EPI is associated with establishment of the first crustal magma chamber in this area, where magma resided for sufficient time to differentiate trachytic compositions. Evidence for this magma chamber is also provided by the syenitic clasts found as accessory lithics within the ignimbrite. The second implication of the EPI ignimbrite is that the trachytic magma was able to produce a large-scale eruption. All subsequent volcanic activity has been limited to the area presently occupied by the main stratovolcano, indicating that the 180 km^3 of products which form the stratovolcano (Worner and Viereck 1990), were erupted since 123 ka, with an average output rate of 1.5 km^3/kyear. The most recent, Holocene deposits are exposed at the top of Mt. Melbourne, where the crater rim is composed of trachytic-rhyolitic pumice fall deposits. Although a precise age was not obtained from these younger summit samples, our data suggest that these deposits are very young (50±70 and 35±22 ka), further suggesting growth of the Mt Melbourne stratocone in Upper Pleistocene–Holocene time (cf. Armstrong 1978).

Magmatic activity of the Mt. Melbourne stratovolcano is bi-modal (Fig. 10), with dominantly explosive products from evolved magmas such as trachytes and rhyolites (EPI ignimbrite and the recent deposits), along with the dominantly effusive eruption of poorly evolved alkali basalts and hawaiites [ARL, ROL and hawaiite scoria cone (SCC) Fms.]. The overlapping compositions of the Edmonson Point trachytes and the Mt.Melbourne summit trachytes suggest a cyclicity of the basalt-trachyte trend. The Harker diagrams variations (Fig. 11; Appendix 8), the observed mineral assemblages and the mineral chemistries (Appendix 7) suggest that the differentiation trend reflects crystal fractionation from alkali basalts to trachytes/rhyolites.

Size of the most recent explosive eruption at Mt Melbourne

Based on composition, texture and depositional characteristics, we have inferred as correlative the most recent pumice fall deposit that drapes the Mt. Melbourne summit crater rim (samples G56 and G79) and the pumice lapilli layer exposed within the ice cap some 16 km to the NNE (sample G62). With just two points, we could not produce an isopach map of this fall deposit. Nevertheless, in view of the extreme limitations offered by the Antarctic environment and the importance of making the most out of available data to constrain the size of the most recent explosive eruption at Mt Melbourne, we propose a line of reasoning, which enables qualitative classification of this eruption as at least as sub-plinian and probably Plinian, based on the tentative reconstruction of the column height able to generate the pumice and lithic grain sizes of sample G62, at 16 km NNE from crater rim.

Prevailing winds in this part of Northern Victoria Land are catabatic winds dominantly from the W and subordinately NW, i.e. from the main Reeves (270°) and Priestly valleys (330°) (Bromwich et al. 1990; Argentini et al. 1995).

Pumice clasts of G62 do float and density is therefore lower than 1,000 kg/m^3. A minimum isopleth area of 100 km^2 can be approximated by if it is assumed that G62 is along a NNE axis of maximum dispersal (which is very unlikely considering the known prevailing wind directions) with a highly eccentric isopleth (0.9 ratio; nine times longer than wide; e.g. Carey and Sigurdsson 1987; Pfeiffer et al 2005). According to calculations given in Carey and Sparks 1986, the 1.5-cm average pumice clast size of G62 can be dispersed by a column 14 km high. This is also consistent with average lithic size of 0.5 cm. By taking into account also the 2 cm maximum pumice clast size and 0.6 cm maximum lithic clast size of G62, it is possible to infer also a wind velocity of up to 20–30 m/s. This is a minimum scenario and allows classification of this eruption as sub-plinian in scale. In a more realistic scenario, taking into consideration prevailing wind directions of the region, the G62 deposit would represent the thickness and grain size of deposits well off-axis within a much larger isopleth with maximum dispersal toward the east or southeast. In this case, a much higher eruption column would be inferred and the eruption classified as Plinian in intensity and of significantly larger magnitude.

Conclusions

We have reconstructed the evolution of the Mt. Melbourne volcanic area using stratigraphy, petrography and geochemistry, and age determinations. In summary:

1. Volcanism in the Mt. Melbourne area started during the Upper Pliocene with formation of the Cape Washington shield volcano; during the Lower and Middle Pleistocene (Random Hills Period and Shield Nunatak Period, respectively), volcanism migrated towards the Transantarctic Mountains, where tens of small, monogenetic scoria cones and lava flows were emplaced over a wide area likely in response to active intra-plate tectonics; in this period, the erupted magmas were predominantly alkali basaltic to hawaiitic;

2. The Upper Pleistocene–Holocene Mt. Melbourne stratovolcano (<123 ka, Mt. Melbourne Period) is associated with the establishment of a crustal magma chamber. Effusive to strombolian eruption styles produced alkali-basaltic and hawaiitic fissure centres, whereas Plinian explosive volcanism is associated with trachytic–rhyolitic compositions, which have also characterised the most recent activity of the volcano; the average eruption rate is 1.5 km^3/ka.

3. Mt. Melbourne must be considered a potentially active volcano (Nathan and Schulte 1968; LeMasurier and Thomson 1990). The outlined evolution of the Mt. Melbourne stratovolcano suggests that intense, potentially Plinian explosive activity is cyclically associated with the evolution of the magma to volatile-rich trachytic–rhyolitic compositions. We suggest that the potential for a renewal of intense explosive activity in the near future must be considered, given that the last eruptions were explosive and associated with the most evolved magma compositions. Although such an eruption may not directly threaten human populations, it could have important effects on the local environment, on global climate (e.g. Sadler and Grattan 1999; Oppenheimer 2003), and on economies in the southern emisphere.

Acknowledgements This work was funded by PNRA 2002–2003 Project 4.4 (coordinator R. Funiciello). The work benefited of comments by J. Gamble and L. Viereck-Gotte on an earlier version and of anonymous reviewers. We also acknowledge J. White and E. Calder for the editorial responsibility. GG thanks P. Pertusati, the alpine guides Palla and Igor and the helicopter pilots Nigel and Steve for the unvaluable and precious help in the field.

References

Antonini P, Civetta L, Orsi G, Piccirillo EM, Bellieni G (1994) The Mount Melbourne and Mount Overlord subprovinces of the McMurdo Volcanic Group (Northern Victoria Land–Antarctica): new geochemical and Sr-isotope data. Terra Antarct 1(1):115–119

Argentini S, Del Buono P, Della Vedova AM, Mastrantonio G (1995) A statistical analysis of wind in TerraNovaBay, Antarctica, for the austral summers 1988 and 1989. Atmos Res 39(1–3):145–156

Armienti P, Tripodo A (1991) Petrologicaphy and chemistry of lavas and comagmatic xenoliths of Mt. Rittmann, a volcano discovered during the IV Italian Expedition in Northern Victoria Land (Antarctica). Mem Soc Geol Ital 46:427–452

Armienti P, Civetta L, Innocenti F, Manetti P, Tripodo A, Villari L, De Vita G (1991) New petrological and geochemical data on Mt. Melbourne volcanic Field, Northern Victoria Land Antarctica (II Italian Antarctic Expedition). Mem Soc Geol Ital 46:397–424

Armstrong RL (1978) K-Ar dating: Late Cenozoic McMurdo Volcanic Group and dry valley glacial history, Victoria Land, Antarctica: New Zealand. J Geol Geophys 21:685–698

Baroni C, Orombelli G (1994) Abandoned penguin rookeries as Holocene paleoclimatic indicators in Antarctica. Geology 22(1):23–26

Beccaluva L, Coltorti M, Orsi G, Saccani A, Siena F (1991a) Nature and evolution of the sub-continental litospheric mantle of Antarctica: evidence from ultramafic xenoliths of the Melbourne Volcanic Province (Northern Victoria Land, Antarctica). Mem Soc Geol Ital 46:353–370

Beccaluva L, Civetta L, Coltorti M, Orsi G, Saccani E, Siena F (1991b) Basanite to tephrite lavas from Melbourne Volcanic Province, Victoria Land, Antarctica. Mem Soc Geol Ital 46:383–395

Behrendt JC (1999) Crustal and lithospheric structure of the West Antarctic Rift System from geophysical investigations—a review. Glob Planet Chang 23:25–44

Bellieni G, Justin Visentin E, Le Maitre RW, Piccirillo EM and Zanettin B (1983) Proposal for a division of the basaltic (B) field of the TAS diagram. IUGS subcommission on the Systematics of Igneous Rocks. Circular no.38, Contribution no.102

Bonnefoi CC, Provost A, Albarède F (1995) The "Daly gap" as a magmatic catastrophe. Nature 378:270–272

Brandelik A (2009) CALCMIN—an EXCEL™ Visual Basic application for calculating mineral structural formulae from electron microprobe analyses. Comput Geosci 35:1540–1551

Branney MJ and Kokelaar P (2002) Pyroclastic density currents and the sedimentation of ignimbrites. In: Branney M.J. & Kokelaar: (eds) Pyroclastic density currents and the sedimentation of ignimbrite Geol Soc Mem 27: 1–138

Bromwich DH, Parish TR, Zorman CA (1990) The confluence zone of intense catabatic winds at Terra Nova Bay, Antarctica, as derived from airborne Sastrugi surveys and mesoscale numerical modeling. J Geophys Res 95:5495–5509

Carey S, Sigurdsson H (1987) The eruption of Vesuvius in A.D. 79: II. Variation in column height and discharge rate. Geol Soc Am Bull 99(2):303–314

Carey S, Sparks RSJ (1986) Quantitative models of the fallout and dispersal of tephra from volcanic eruption columns. Bull Volcanol 48:109–125

Cas RAF (1992) Submarine volcanism: eruption styles, products, and relevance to understanding the host rock successions to volcanic-hosted massive sulfide deposits. Econ Geol 87(511):541

Cas RAF, Wright JV (1987) Volcanic successions: modern and ancient. Chapman & Hall, London, p 528

Cremisini C, Gianelli G, Mussi M, Torcini S (1991) Geochemistry and isotope chemistry of surface waters and geothermal manifestations at Terra Nova Bay (Victoria Land, antartica). Mem Soc Geol Ital 46:463–475

D'Amico C, Innocenti F and Sassi FP (1989) Magmatismo e Metamorfismo, Utet, 536p

Di Nicola L, Strasky S, Schlüchter C, Salvatore MC, Akçar N, Kubik PW, Christl M, Kasper HU, Wieler R, Baroni C (2009) Multiple cosmogenic nuclides document complex Pleistocene exposure history of glacial drifts in Terra Nova Bay (northern Victoria Land, Antarctica). Quat Res 71:83–92

Dunbar NW, McIntosh WC, Esser RP (2008) Physical setting and tephrochronology of the summit caldera ice record at Mount Moulton, West Antarctica. Geol Soc Am Bull 120:796–812. doi:10.1130/B26140.1

Fitzgerald PG, Sandford M, Barrett PJ, Gleadow AJW (1987) Asymmetric extension associated with uplift and subsidence in the Transantarctic Mountains and Ross Embayment. Earth Planet Sci Lett 81:67–78

Harrington HJ (1958) Nomenclature of rock units in the Ross Sea Region, Antarctica. Nature 182(4631):290

Hornig I, Wörner G, Zipfel J (1991) Lower crustal and mantle xenoliths from the Mt. Melbourne Volcanic Field, Northern Victoria Land, Antarctica. Mem Soc Geol Ital 46:337–352

Irvine TN, Baragar WRA (1971) A guide to the chemical classification of the common volcanic rocks. Can J Earth Sci 8:523–548

Jacobs SS (1992) Is the Antarctic sheet growing? Nature 360:29–33

Keys JR, McIntosh WC, Kyle PR (1983) Volcanic activity of Mount Melbourne, Northern Victoria Land. Antarct J US 18:10–11

Kuno H (1966) Lateral variation of basalt magma types across continental margins and island arcs. Bull Volcanol 29:195–222

Kyle PR (1990a) Melbourne Volcanic Province. In: LeMasurier WE and Thmson JW (eds), 1990. Volcanoes of the Antarctic plate and southern oceans. Am Geophys Union, Antarct Res Series 48: 48–52

Kyle PR (1990b) McMurdo Volcanic Group, Western Ross Embayment. In: LeMasurier WE and Thmson JW (eds), 1990. Volcanoes of the Antarctic Plate and Southern Oceans. Am Geophys Union, Antarct Res Series 48: 19–145

Kyle PR, Cole JW (1974) Strucutral controls of volcanism in the McMurdo volcanic Group, McMurdo Sound, Antarctica. Bull Volcanol 38:16–35

Lanzafame G, Villari L (1991) Structural evolution and volcanism in Northern Victoria Land (Antarctica): data from Mt. Melbourne–Mt. Overlord–Malta Plateau Region. Mem Soc Geol Ital 46:371–381

Le Bas MJ, Streckeisen A (1991) The IUGS systematics of igneous rocks. J Geol Soc Lond 148:825–833

Le Bas MJ, LeMaitre RW, Streckeisen A, Zanettin B (1986) A chemical classification of volcanic rocks based on the total alkali-silica diagram. J Petrol 27:745–750

LeMaitre RW (ed) (2002) Igneous rocks: a classification and glossary of terms: recommendations of the International Union of Geological Sciences. Subcommission on the Systematics of Igneous Rocks. Cambridge University Press, Cambridge

LeMasurier WE and Thomson JW (eds) (1990) Volcanoes of the Antarctic plate and southern oceans. Am Geophys Union, Antarct Res Series 48:512

Lesti C, Giordano G, Salvini F, Cas R (2008) Volcano tectonic setting of the intraplate, Pliocene–Holocene, Newer Volcanic Province (southeast Australia): role of crustal fracture zones. J Geophys Res 113:B07407. doi:10.1029/2007JB005110

Lyon GL (1986) Stable isotope stratigraphy of ice cores and the age of the last eruption at Mt.Melbourne, Antarctica. NZJ Geol Geophys 29(1):135–138

Lyon GL, Giggenbach WF (1974) Geothermal activity in Victoria Land, Antarctica. NZ J Geol Geophys 17:511–521

Martin A, Cooper A, Dunlap W (2010) Geochronology of Mount Morning, Antarctica: two-phase evolution of a long-lived trachyte–basanite–phonolite eruptive center. Bull Volcanol 72(3):357–371

Matchan E, Phillips D (2011) New 40Ar/39Ar ages for selected young (<1 Ma) basalt flows of the Newer Volcanic Province, southeastern Australia. Quat Geochronol 6:356–358

McPhie J, Doyle M and Allen R (1993) Volcanic textures: a guide to the interpretation of textures in volcanic rocks. Centre for Ore Deposit and Exploration Studies, University of Tasmania, 198 p

Min K, Mundil R, Renne PR, Ludwig KR (2000) A test for systematic errors in 40Ar/39Ar geochronology through comparison with U–Pb analysis of a 1.1 Ga rhyolite. Geochim Cosmochim Acta 64:73–98

Müller P, Schmidt-Thome M, Kreuzer H, Tessensohn F, Vetter U (1991) Cenozoic Peralkaline magmatism at the western margin of the Ross Sea, Antarctica. Mem Soc Geol Ital 46:315–336

Nathan S, Schulte FJ (1967) Recent thermal and volcanic activity on the Mt. Melbourne, Northern Victoria Land, Antarctica. NZ J Geol Geophys 10:422–430

Nathan S, Schulte FJ (1968) Geology and petrology of the Campbell–Aviator Divide, Northern Victoria Land, Antarctica. Part I: Post Paleozoic rocks. NZ J Geol Geophys 11:940–975

Oppenheimer C (2003) Climatic, environmental and human consequences of the largest known historic eruption: Tambora volcano (Indonesia) 1815. Prog Phys Geogr 27:230–259

Orombelli G, Baroni C, Denton GH (1991) Late Cenozoic galcial history of the Terra Nova Bay region, Northern Victoria Land, Antarctica. Geogr Fis Dinamica Quaternaria 13:139–163

Pfeiffer T, Costa A, Macedonio G (2005) A model for the numerical simulation of tephra fall deposits. J Volcanol Geotherm Res 140:273–294

Phillips G, Wilson CJL, Phillips D, Szczepanski S (2007) Thermochronological (40Ar/39Ar) evidence for Early Palaeozoic basin inversion within the southern Prince Charles Mountains, East Antarctica: implications for East Gondwana. J Geol Soc 164:771–784

Renne PR, Swisher CC, Deino AL, Karner DB, Owens TL, DePaolo DJ (1998) Intercalibration of standards, absolute ages and uncertainties in 40Ar/39Ar dating. Chem Geol 145:117–152

Renne PR, Mundil R, Balco G and Min K (2009) Simultaneous determination of 40 K decay constants and age of the Fish Canyon sanidine 40Ar/39Ar standard. GSA Annual Meeting, Portland, abstract 160–3

Rocchi S, Storti F, Di Vincenzo G, and Rossetti F (2003) Intraplate strike-slip tectonics as an alternative to mantle plume activity for the Cenozoic rift magmatism in the Ross Sea region, Antarctica: in Storti, F, Holdsworth, R.E. and Salvini, F. (eds), Intraplate Strike-Slip Deformation Belts, Geol Soc London, Special Publication 210: 145–158

Rossetti F, Storti F, Salvini F (2000) Cenozoic non-coaxial transtension along the western shoulder of the Ross Sea, Antarctica, and the emplacement of McMurdo dyke arrays. Terra Nova 12:60–66

Sadler J, Grattan JP (1999) Volcanoes as agents of past environmental change. Glob Planet Chang 21:181–196

Salvini F, Brancolini G, Busetti M, Storti F, Mazzarini F, Coren F (1997) Cenozoic geodynamics of the Ross Sea Region, Antarctica: crustal extension, intraplate strike-slip faulting and tectonic inheritance. J Geophys Res 102:24669–24696

Smellie JL, Chapman MG (2002) Volcano–ice interaction on Earth and Mars. Geol Soc Lond 202:437, Special Publication

Steiger RH, Jager E (1977) Subcommission on geochronology: convention on the use of decay constants in geo- and cosmochronology. Earth Planet Sci Lett 36:359–362

Stewart DC, Thornton CP (1975) Andesites in oceanic regions. Geology 3:565–568

Storti F, Rossetti F, Laufer AL, Salvini F (2006) Consistent kinematic architecture in the damage zones of intraplate strike–slip fault systems in North Victoria Land, Antarctica and implications for fault zone evolution. J Struct Geol 28:50–63

Wilch TI, McIntosh WC, Dunbar NW (1999) Late Quaternary volcanic activity in Marie Byrd Land:Potential 40 Ar/39Ar-dated time horizons in West Antarctic ice and marine cores. Geol Soc Am Bull 111(10):1563–1580

Wörner G, Orsi G (1990) Volcanic geology of Edmonson Point, Mt. Melbourne Volcanic Field, North Victoria Land, Antarctica. Polarforschung 60(2):84–86

Wörner G, Viereck L (1989) The Mt. Melbourne volcanic field (Victoria Land, Antarctica). I Field observations. Geol Jahrb E38:369–393

Worner G and Viereck L (1990) Mount Melbourne. In: LeMasurier WE and Thmson JW (eds), 1990, Volcanoes of the Antarctic Plate and Southern Oceans. Am Geophys Union, Antarct Res Series 48: 72–78

Wörner G, Viereck L, Hertogen J, Niephaus H (1989) The Mt. Melbourne Field (Victoria Land, Antarctica) II. Geochemistry and magma genesis. Geol Jahrb E38:395–433

Wysoczanski RJ, Gamble JA (1992) Xenoliths from the Volcanic Province of West Antarctica and implications for lithospheric structure and processes. In: Yoshida Y, Kaminuma K, Shiraishi K (eds) Recent progress in Antarctic Earth Science. Terra Science Publication, Tokyo, pp 273–277

Yavuz F (2007) WinAmphcal: a Windows program for the IMA-04 amphibole classification. Geochem Geophys Geosyst 8:Q01004. doi:10.1029/2006GC001391